Facing the Future: Effects of Short-Term Climate Extremes on Isoprene-Emitting and Nonemitting Poplar¹

Elisa Vanzo, Werner Jud, Ziru Li², Andreas Albert, Malgorzata A. Domagalska, Andrea Ghirardo, Bishu Niederbacher, Juliane Frenzel, Gerrit T.S. Beemster, Han Asard, Heinz Rennenberg, Thomas D. Sharkey, Armin Hansel, and Jörg-Peter Schnitzler*

Helmholtz Zentrum München, Research Unit Environmental Simulation at the Institute of Biochemical Plant Pathology, 85764 Neuherberg, Germany (E.V., A.A., A.G., B.N., J.-P.S.); Institute for Ion Physics and Applied Physics, University of Innsbruck, 6020 Innsbruck, Austria (W.J., A.H.); Department of Biochemistry and Molecular Biology, Michigan State University, East Lansing, Michigan 48824 (Z.L., T.D.S.); Laboratory for Molecular Plant Physiology and Biotechnology, Department of Biology, University of Antwerp, 2020 Antwerp, Belgium (M.A.D., G.T.S.B., H.A.); and Institute of Forest Sciences, University of Freiburg, 79110 Freiburg, Germany (J.F., H.R.)

ORCID IDs: 0000-0003-4267-0435 (W.J.); 0000-0002-0582-2674 (A.A.); 0000-0001-6014-053X (G.T.S.B.); 0000-0001-7469-4074 (H.A.); 0000-0001-6224-2927 (H.R.); 0000-0002-9825-867X (J.-P.S.).

Isoprene emissions from poplar (Populus spp.) plantations can influence atmospheric chemistry and regional climate. These emissions respond strongly to temperature, $[CO_2]$, and drought, but the superimposed effect of these three climate change factors are, for the most part, unknown. Performing predicted climate change scenario simulations (periodic and chronic heat and drought spells [HDSs] applied under elevated $[CO_2]$), we analyzed volatile organic compound emissions, photosynthetic performance, leaf growth, and overall carbon (C) gain of poplar genotypes emitting (IE) and nonemitting (NE) isoprene. We aimed (1) to evaluate the proposed beneficial effect of isoprene emission on plant stress mitigation and recovery capacity and (2) to estimate the cumulative net C gain under the projected future climate. During HDSs, the chloroplastidic electron transport rate of NE plants became impaired, while IE plants maintained high values similar to unstressed controls. During recovery from HDS episodes, IE plants reached higher daily net CO_2 assimilation rates compared with NE genotypes. Irrespective of the genotype, plants undergoing chronic HDSs showed the lowest cumulative C gain. Under control conditions simulating ambient $[CO_2]$, the C gain was lower in the IE plants than in the NE plants. In summary, the data on the overall C gain and plant growth suggest that the beneficial function of isoprene emission in poplar might be of minor importance to mitigate predicted short-term climate extremes under elevated $[CO_2]$. Moreover, we demonstrate that an analysis of the canopy-scale dynamics of isoprene emission and photosynthetic performance under multiple stresses is essential to understand the overall performance under proposed future conditions.

Climate change will lead to an increase in global temperatures of at least 2°C in the near future (IPCC, 2014). There is at present substantial evidence that this

climate change is leading to an increase in the frequency and intensity of extreme events such as heat and drought waves (Feyen and Dankers, 2009; Fischer and Schär, 2010; Perkins et al., 2012; Thornton et al., 2014), creating a sequence of recurring stress and recovery cycles for plants. Coumou and Rahmstorf (2012) showed that, in the last 15 years, five extreme heat wave events have occurred worldwide, four of which were observed also in Europe. Interactions between heat and drought under predicted elevated [CO₂] (IPCC, 2014) generate complex, often nonadditive physiological responses. Such effects cannot be predicted by singlefactor analyses and highlight the importance of carrying out controlled, multistress scenarios to investigate plant performance under future climate conditions (Clausen et al., 2011; Alemayehu et al., 2014).

Photosynthesis, respiration, and photorespiration are the three dominating processes determining carbon (C) exchange and C metabolism in plants (Bauwe et al., 2010; Mahecha et al., 2010). In addition, the emission of biogenic volatile organic compounds (VOCs) contributes to the overall C exchange of plants, with isoprene being the most abundant volatile compound that is

¹ This work was supported by the European Science Foundation Eurocores program EuroVOL within the joint research project MOMEVIP (to H.A., T.D.S., A.H., and J.-P.S.), by the German Ministry of Education and Research (PROBIOPA project to H.R. and J.-P.S.), by the Belgian Fund for Scientific Research (grant no. GA13511N to M.A.D., G.T.S.B., and H.A.), and by the Austrian Science Funds (project no. I655–B16 to W.J. and A.H.).

² Present address: Benson Hill Biosystems, 1100 Corporate Square Drive, St. Louis, MO 63132.

^{*} Address correspondence to jp.schnitzler@helmholtz-muenchen.de. The author responsible for distribution of materials integral to the findings presented in this article in accordance with the policy described in the Instructions for Authors (www.plantphysiol.org) is: Jörg-Peter Schnitzler (jp.schnitzler@helmholtz-muenchen.de).

J.-P.S., H.A., A.H., T.D.S., G.T.S.B., and H.R. conceived the original research plan; A.A. and J.-P.S. supervised the experiments; E.V., W.J., Z.L., and M.A.D. performed most of the experiments; B.N., A.A., and A.G. provided technical assistance to E.V.; E.V., W.J., Z.L., M.A.D., A.A., and J.F. analyzed the data; E.V. wrote the article with contributions of all the authors; J.-P.S. supervised and complemented the writing. www.plantphysiol.org/cgi/doi/10.1104/pp.15.00871

released by vegetation, in particular by forest ecosystems (Guenther et al., 2006). Due to its high reactivity, isoprene can significantly influence the oxidative capacity of the troposphere as well as cloud formation, with important consequences for air quality, climate, ecosystem processes, and even human health (Bell et al., 2007; Ashworth et al., 2012).

From a plant's perspective, isoprene is an important bioactive hydrocarbon, participating in the mitigation of a wide range of abiotic stresses (Loreto and Schnitzler, 2010), in particular transient episodes of high temperature and light (Monson et al., 1992; Sharkey et al., 2001; Behnke et al., 2007, 2010b), oxidative stress (Loreto and Velikova, 2001; Affek and Yakir, 2002; Vickers et al., 2009), and drought (Brilli et al., 2007).

In terms of C and energy, isoprene biosynthesis is a costly investment for the plant (Sharkey and Yeh, 2001; Ghirardo et al., 2011) and is biochemically (Schnitzler et al., 2005; Rasulov et al., 2010; Way et al., 2011; Monson et al., 2012) and transcriptionally (Mayrhofer et al., 2005; Wiberley et al., 2009) under the control of environmental factors such as light, temperature, and [CO₂]. Isoprene synthesis is light dependent (Loreto and Sharkey, 1993); however, emissions can become uncoupled from photosynthesis under stress that impairs net CO₂ assimilation (A) and makes plants rely on alternative (old) C sources (Affek and Yakir, 2003; Brilli et al., 2007; Ghirardo et al., 2011; Trowbridge et al., 2012). While isoprene biosynthesis and emission correlate with fluctuations in leaf temperature (Monson et al., 1992; Singsaas and Sharkey, 1998), increases in atmospheric [CO₂] have a more ambiguous effect on isoprene emission. At the leaf level, isoprene biosynthesis and its consequent emission in poplar (Populus spp.) is inhibited in elevated [CO₂] environments (Rosenstiel et al., 2003; Way et al., 2011), but the inhibitory effect is reduced at temperatures higher than 30°C (Potosnak et al., 2014). Canopy-scale flux measurements report enhanced isoprene emission at high [CO₂] due to strongly enhanced canopy leaf dry mass and leaf area index (Sun et al., 2013). Thus, for predicting future isoprene emissions, one has to consider not only the direct effects of global drivers on the isoprene emission capacity (e.g. light, [CO₂], and temperature) but also indirect effects resulting from changes in the overall net primary productivity (Constable et al., 1999; Arneth et al., 2008) and the impact of stress (e.g. drought).

The impact of drought alone on the amount of isoprene emission depends on the timing and severity of the stress (Brüggemann and Schnitzler, 2002; Brilli et al., 2007, 2013; Fortunati et al., 2008; Tattini et al., 2014) and the cooccurrence of other abiotic stressors (e.g. temperature; Centritto et al., 2011). Previous cuvette-based measurements demonstrated that, under standard conditions (fixed light and leaf temperature), the capacity for isoprene formation is sustained under mild drought stress but begins to decline when water scarcity becomes more severe or prolonged (Pegoraro et al., 2004; Brilli et al., 2007; Fortunati et al., 2008). However, how these effects on isoprene emission emerge at the

canopy scale and under fluctuating ambient climatic conditions is unknown.

The predicted increases in climate extremes, such as summer droughts and concomitant heat spells, threaten plant growth and fitness (Rennenberg et al., 2006). This threat is particularly true when stressful climatic conditions recur within short intervals, as plant fitness depends not only on tolerance during the stress but also on the ability to recover rapidly and completely after these events. The rate and extent of photosynthetic recovery have been examined in several studies (Kirschbaum, 1988; Gallé and Feller, 2007; Correia et al., 2014). However, information regarding the recovery of VOC emission following environmental stress is scarce (Pegoraro et al., 2004; Fortunati et al., 2008; Centritto et al., 2011) and virtually lacking when plants experience multiple environmental stresses. Improved mitigation of oxidative stress (via antioxidants) and the capacity to preserve chloroplast membrane stability during stress phases are crucial for a fast and complete recovery (Mittler and Zilinskas, 1994; Sales et al., 2013). In this context, the ascribed antioxidative and membrane-stabilizing properties of isoprene (Vickers et al., 2009; Velikova et al., 2011) may abate membrane damage during the occurrence of stress, paving the way for a more rapid and complete recovery.

Poplar, a strong isoprene emitter, is a widely used woody model organism (Wullschleger et al., 2002; Brunner et al., 2004; Tuskan et al., 2006). Poplars are fast-growing tree species that are globally used in plantation forestry for cellulose production or more recently in intensive short-rotation coppice for bioenergy generation (Aylott et al., 2008). In the context of climate change policy to reduce greenhouse gas emissions, the cultivation of poplar in short-rotation coppice is close to C neutral (Aylott et al., 2008). However, as a fast-growing pioneer tree species, poplars are hygrophilic plants with high transpiration rates (Allen et al., 1999), and their productivity depends strongly on water availability (Tschaplinski et al., 1998). In view of the predicted water scarcity (IPCC, 2014) and the increase in the poplar plantation area, an advanced understanding of the water-use efficiency (WUE) of poplar in water-limited environments is essential.

In this study, we aimed to assess the effects of predicted climate change on the photosynthetic performance, isoprene emission, plant growth, and overall fitness of poplar grown in well-controlled phytotron chambers. We designed the experimental scenarios based on the fourth IPCC report (IPCC, 2007), being consistent with the latest report (IPCC, 2014) and focused on projections of the summer climate in the short term (until 2050) in central Europe: elevated atmospheric [CO₂], periodic (short-term) and chronic (long-term) high-temperature episodes with concomitant reduction in precipitation, and intermittent, short phases of recovery. Using Grey poplar (Populus × canescens) wild type and well-established transgenic genotypes, which are almost completely suppressed in isoprene emission (Behnke et al., 2007, 2012), we aimed to address the following questions. (1) What are the dynamics of photosynthesis and VOC emissions under the different climate scenarios? (2) Is the ability to tolerate stress and to recover different between short-term and long-term heat and drought spells (HDSs), and what are the costs (in terms of C gain) that poplars will pay under the projected future climate? (3) Is the trait isoprene emission essential for poplar to adapt to fast-changing environmental extremes and to influence the recovery after stress?

RESULTS

Photosynthetic Parameters under Climate Change Scenarios Measured at the Plant Scale

We studied the photosynthetic performance of isoprene-emitting (IE) and nonemitting (NE) plants under averaged present-day and projected future climates (Fig. 1) by measuring the net plant (canopy) CO₂ flux (i.e. the net ecosystem exchange [NEE]) and evapotranspiration rate (Fig. 2) of the plants. NEE was equal in IE and NE poplars in the control scenarios (ambient and elevated [CO₂]); overall, elevated [CO₂] increased the NEE (P = 0.001). HDSs significantly decreased (all P values are given in Supplemental Table S1) the NEE under PS and CS in both IE and NE plants (Fig. 2) compared with plants that were grown in the control chambers under ambient and enhanced [CO₂]. After three cycles (PS) or 22 d (CS) of heat and drought, the NEE decreased to 43% and 35%, respectively, compared with the ambient control, with no differences between IE and NE genotypes. At this time point (S3; see Fig. 1 legend), the irrigation was the lowest (Supplemental Fig. S1C). HDSs also affected the evapotranspiration rates, showing similar dynamics to those that were observed for NEE but with a much more pronounced decline (Fig. 2B).

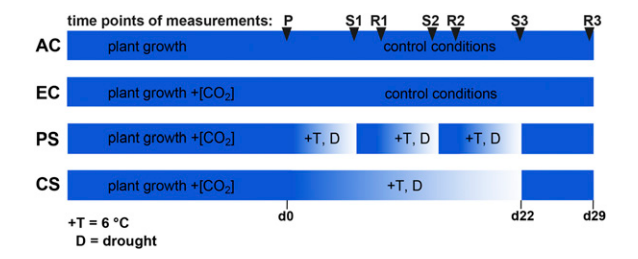


Figure 1. Schematic overview of the four climate change scenarios and measurement time points. Scenarios are as follows: AC, ambient $[CO_2]$; EC, elevated $[CO_2]$; PS, periodic stress; CS, chronic stress. Time points of measurements are as follows: P, prestress; S1, stress cycle 1; R1, recovery cycle 1; S2, stress cycle 2; R2, recovery cycle 2; S3, stress cycle 3; R3, recovery cycle 3. Relative time is indicated along the bottom and spans from day 0 (d0) to day 29 (d29), where day 0 represents the day prior to the start of the first HDS (PS) and the beginning of the progressive drought (CS). Before day 0, the plants were cultivated for 25 d under AC and EC control climates to adjust growth and physiology. At day 0, the plants were 8.5 weeks old.

During recovery, IE plants reached significantly higher NEE rates compared with those of NE plants under both stress scenarios (P = 0.016 in PS and P = 0.042 in CS). Compared with the NEE rates of poplars under control conditions, the NEE in PS was 95% and 53% higher in IE and NE plants, respectively. In CS, the increase during R3 was 36% higher in IE plants and 25% higher in NE plants (P < 0.05 for all).

The ETR, a measure of the photosynthetic performance in the light-adapted state, was similar in IE and NE plants that were grown under present and future [CO₂] when no HDSs were applied. The application of periodic HDSs reduced the ETR in the NE poplars during each stress cycle, while the ETR of the IE plants was maintained at control levels (or even slightly increased) during the first and second stress cycles and decreased in the last cycle (P = 0.001; Fig. 2). The ETR in the NE plants was significantly different from that of the IE plants during the first ($\dot{P} = 0.024$), second (P <0.001), and third (P = 0.014) stress cycles. In CS, ETR began to decrease in NE plants at day 8 of HDSs, reaching a minimum value of 73 μ mol m⁻² s⁻¹ at day 22, while ETR in IE plants stayed at the control level over the entire experiment. The difference in the ETR between IE and NE plants became statistically significant at day 14 of progressive drought (S2). Similar to the PS scenario, a few days of rewatering and reduced temperature were sufficient to fully recover the ETR in the NE genotype, which reached the same value as that of the IE plants (approximately 82 μ mol m⁻² s⁻¹), irrespective of treatment.

Overall Plant VOC Fluxes under Climate Change Scenarios

The simulation of extreme events (PS and CS) showed dramatically increased net isoprene fluxes per leaf area (LA; nmol isoprene $m^{-2} s^{-1}$) during HDSs at the plant level from IE plants (Fig. 3A). In both of these stress scenarios, during HDSs, the daily sum of isoprene fluxes was 9 times greater than that of poplars growing under unstressed conditions, with a significant increase with each stress cycle (PS) and when the stress progressed in the CS scenario. Under enhanced [CO₂], the isoprene fluxes from the IE plants were slightly lower compared with those of the plants that were grown throughout the entire experimental period under present-day [CO₂] but were statistically significantly lower when the measurements were performed at the leaf level under standard conditions (P = 0.019; Table I). We also calculated the isoprene emission per plant (nmol isoprene s⁻¹ plant⁻¹). This calculation did not change the picture we obtained from the LA base. Here, the increase in the isoprene flux during HDSs was up to 7 times greater than that of controls. Under enhanced [CO₂], the isoprene flux per plant was also slightly lower than that under ambient [CO₂]. The isoprene emission in IE genotypes showed maximal emissions around midday (Supplemental Fig. S2), while the NE plants showed

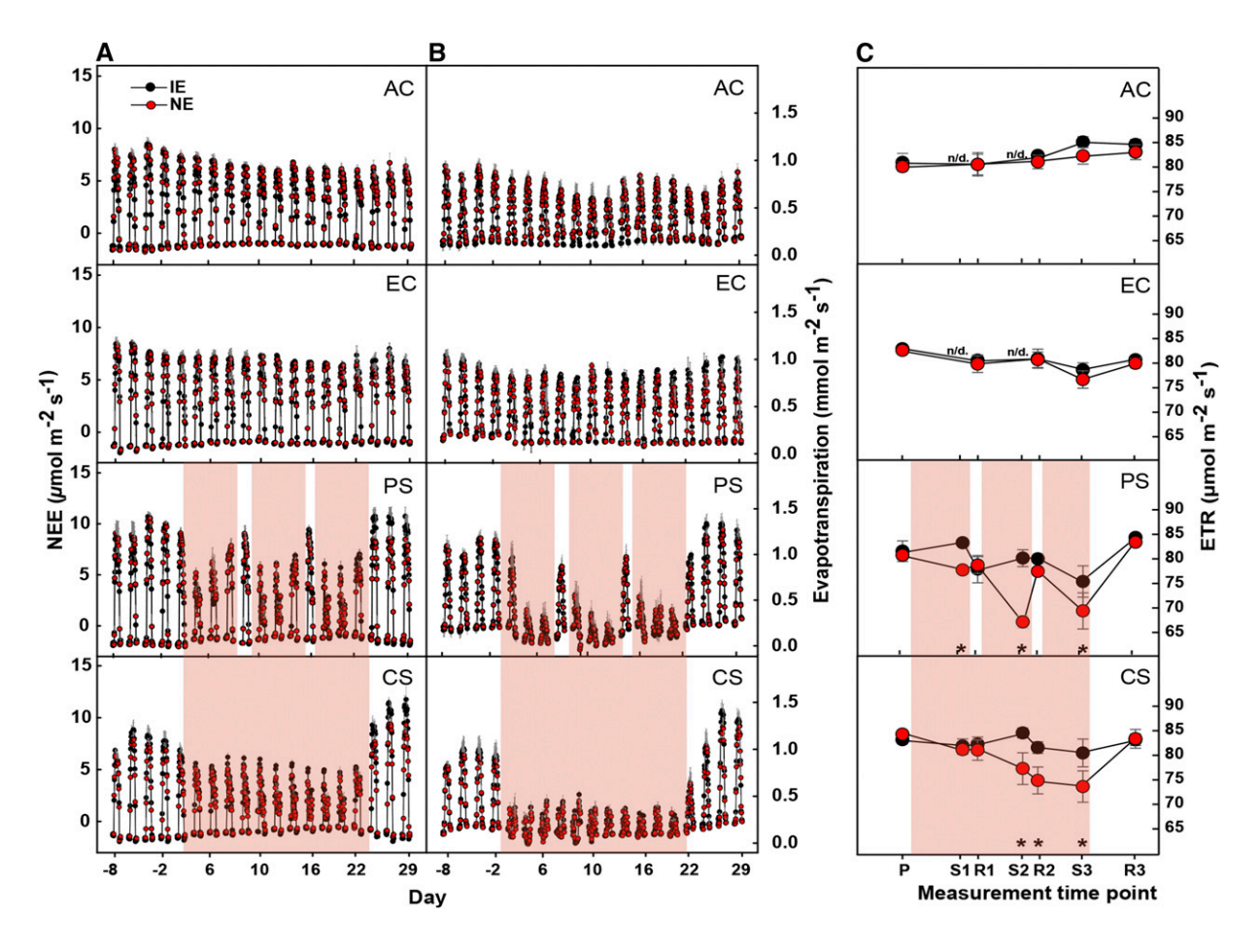


Figure 2. NEE (A), evapotranspiration (B), and electron transport rate (ETR; C) in IE (black circles) and NE (red circles) poplar genotypes. Plant-level NEE and evapotranspiration values for each scenario are given as hourly means of $n=4\pm sE$. ETR was measured on leaf 8 below the apex at the indicated time points. HDSs are highlighted in red. Asterisks indicate significant differences (P < 0.05) between IE and NE plants within each scenario (in addition, P values are given in Supplemental Table S1); n/d, no data. The PS and CS scenarios were performed under elevated [CO₂].

isoprene fluxes of less than 5% compared with IE plants (Fig. 3A).

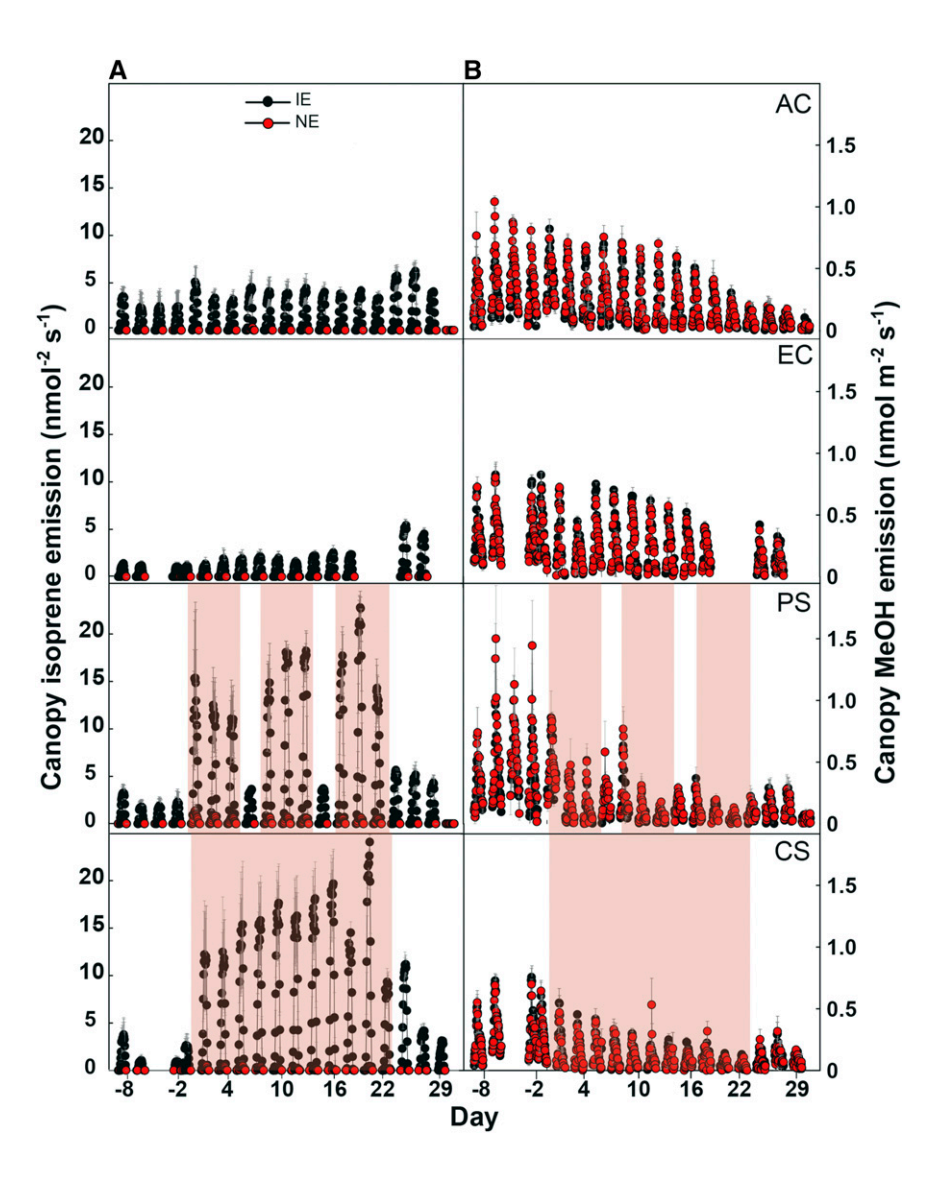
The emission of lipoxygenase (LOX) products (mass-to-charge ratio = 99 [indicated as m99 hereafter] and m101; Supplemental Fig. S3), methyl vinyl ketone (MVK) and/or methacrolein (MACR; both m71), could not be detected. In IE plants, we detected as m71 the double isotope $^{13}\mathrm{C}$ of isoprene (i.e. $^{13}\mathrm{C}_2^{\ 12}\mathrm{C}_3\mathrm{H}_8$), which represents 0.305% of the isoprene emissions at m69 (Supplemental Fig. S3A). Monoterpenes (m137), which are primarily emitted by young, immature poplar leaves (Ghirardo et al., 2011), were detected in trace amounts, particularly at the beginning of the experiment, whereas sesquiterpenes (m205) were never detected (data not shown).

In addition to isoprene, MeOH was the second most abundant VOC. We used the emission of this compound as an indicator of leaf growth (Hüve et al., 2007). Generally, the emission of MeOH decreased toward the end of the experiment (Fig. 3B) and showed no difference between the IE and NE plants. Immediately after the

onset of periodic or chronic HDSs, the MeOH emission started to decline in both IE and NE plants (Fig. 3B). In the PS scenario, MeOH emission recovered from HDSs after the first and was much weaker after the second stress cycle. Under the CS scenario, the emission of MeOH decreased constantly (Fig. 3B). At the diurnal time scale, MeOH emission always peaked in the morning hours (Supplemental Fig. S2), most likely as a consequence of stomatal opening (Niinemets et al., 2004; Hüve et al., 2007), and decreased constantly until the evening.

Because plant primary and secondary metabolism are both temperature dependent (Monson et al., 1992; Way and Yamori, 2014), we monitored the temperature of light-exposed leaves in the scenarios weekly by infrared thermography (Supplemental Fig. S4). Under unstressed conditions (time point P in all scenarios), the leaf temperature was slightly lower than the scenario air temperature (Supplemental Fig. S4B, black dashed line). However, during HDSs, when leaf cooling by transpiration diminishes as a consequence of stomatal closure (Fig. 2; Table I), the leaf temperatures in both of

Figure 3. Overall plant isoprene emission (A) and methanol (MeOH) emission (B) from IE (black circles) and NE (red circles) poplars in the four scenarios. HDSs are highlighted in red. The data are presented as hourly means of $n = 4 \pm \text{s}$ E. The PS and CS scenarios were performed under elevated [CO₂].



the genotypes were 3°C to 4°C higher than the scenario air temperature (Supplemental Fig. S4).

Impact of Climate Change Scenarios on the Plant Water Status and Cell Growth

To noninvasively monitor the water status of the leaves under the different scenarios, we assessed the relative water content (RWC) in young (no. 4, from apex), fully emerged (no. 8), and older (no. 12) leaves throughout the duration of the experiment by measuring the leaf near-infrared reflectance and calculating the moisture stress index (MSI; Hunt and Rock, 1989; Ceccato et al., 2001). The MSI was well correlated with the RWC of Grey poplar leaves during drying ($r^2 = 0.73$, P < 0.001; Supplemental Fig. S5) and was thus a useful indicator of the leaf RWC. Both IE and NE plants had similar RWC across the scenarios and leaf age classes (Fig. 4A). At the time points R2, S3, and R3, the RWC

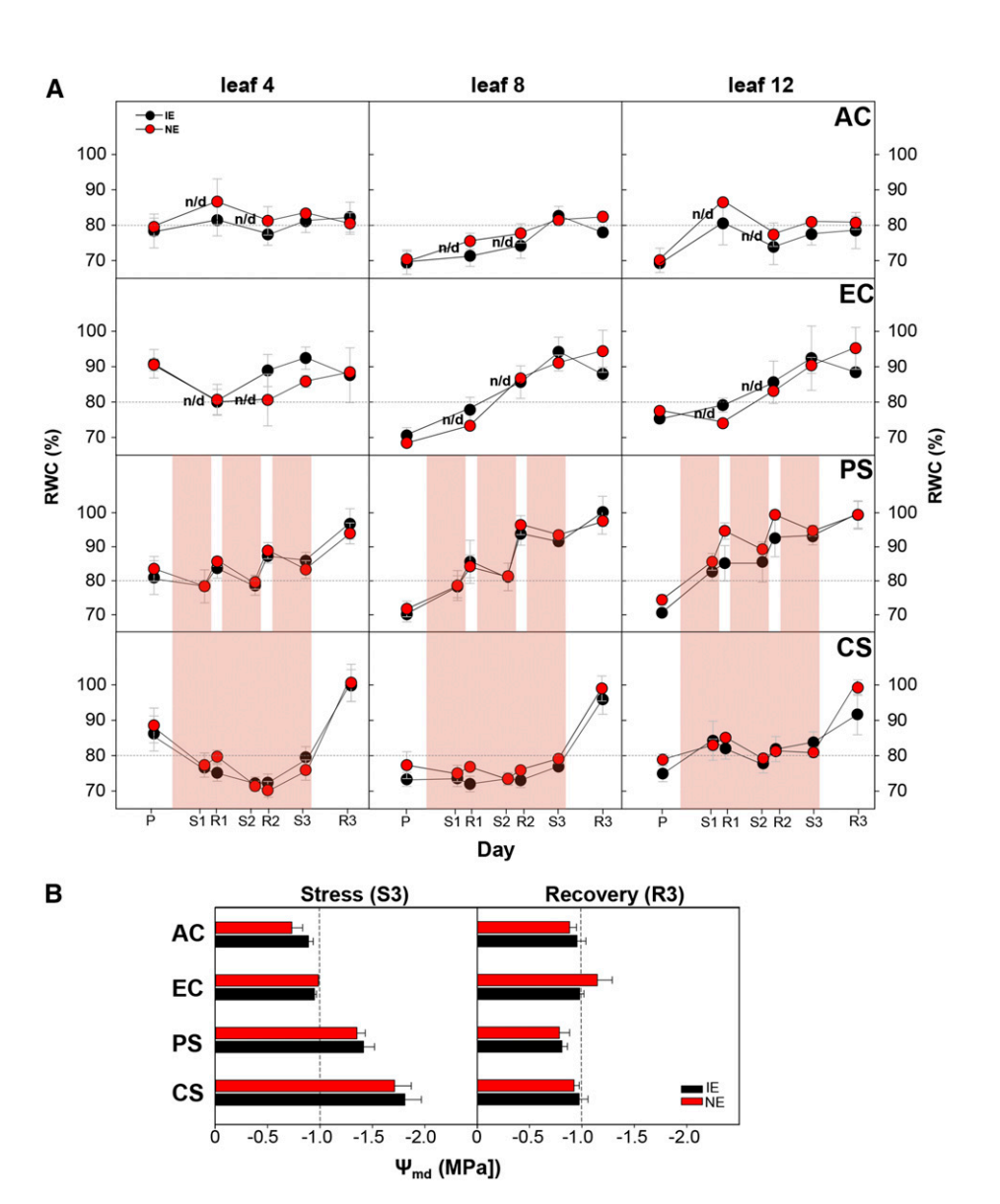
was 5% to 10% higher under elevated [CO₂] compared with that under ambient [CO₂] atmosphere. Plants in the two stress scenarios displayed a remarkable difference in the time course of the RWC. The plants in the PS scenario maintained a high leaf RWC in each leaf age class, with an increase from each recovery cycle to the next (R1, R2, and R3). In the CS scenario, the RWC decreased in the young leaves (no. 4) as HDSs continued or was maintained at prestress levels in leaves 8 and 12. Rewatering induced a distinctive increase in the RWC in all of the leaf age classes in both of the stress scenarios, but the rate of increase almost doubled in CS compared with PS (Fig. 4A). As a classical measure of the water status, we also analyzed the shoot water potential (midday) on a subset of plants at S3 and R3 (Fig. 4B). At S3, both of the genotypes exhibited significantly reduced water potentials compared with those of control plants (P < 0.001, all). Compared with PS, the water potentials under chronic water scarcity were significantly lower (P = 0.002), indicative of more

 Table I. Leaf-level measurements of photosynthetic parameters and isoprene emission

different scenarios (AC, EC, PS, and CS). Gas-exchange measurements were performed at maximum stress (S3) and after 7 d of recovery (R3). Leaf-level cuvette measurements of gas exchange and isoprene emission were performed under steady-state standard conditions (30°C leaf temperature and 1,000 μ mol photons m⁻² s⁻¹). [CO₂] in the cuvette was set as in the respective scenario. Boldface values indicate significant differences between the lines in the same scenario and time point. All effects were regarded as significant at P < 0.05. The PS and CS scenarios were also mitochondrial respiration in the dark (R_d), isoprene emission rate (J), and percentage of photosynthetic C emitted as isoprene (C%) are shown for IE and NE poplar plants grown in the four Main scenario effects were tested with one-way ANOVA within each time point (S3 or R3) and are indicated by different letters (lowercase letters for IE plants and uppercase letters for NE plants). Transpiration rate in the light (E), A, WUE, stomatal water vapor conductance (g,), intercellular [CO2] (c,), ratio of intracellular to extracellular [CO2] (Ratio), transpiration rate in the dark (E,), performed under elevated [CO,]

perioritica ariaci cievatea [502].		1 000	22.									
Time Point Scenario Line	Scenario	Line	E	А	WUE	SS	c,	Ratio	$E_{ m d}$	$R_{ m d}$	I	%D
			$mmol m^{-2} s^{-1}$	$\mu mol \ m^{-2} \ s^{-1}$	μ mol mmol ⁻¹	$mol \ m^{-2} \ s^{-1}$	$\mu L L^{-1}$		$mmol \ m^{-2} \ s^{-1}$	$\mu mol \ m^{-2} \ s^{-1}$	$nmol \ m^{-2} \ s^{-1}$	
S3	AC	ш	$3.79 \pm 0.5a$	$13.09 \pm 2.2a$	$3.69 \pm 0.4a$	$0.125 \pm 0.020a$	$172 \pm 19ab$	$0.45 \pm 0.0a$	$1.58 \pm 0.6a$	$0.96 \pm 0.2a$	$30.99 \pm 8.4ab$	$1.13 \pm 0.1a$
		뿔	$2.76 \pm 0.6A$	9.50 ± 0.44	3.88 ± 0.64	$0.088 \pm 0.02A$	$168 \pm 23AB$	$0.45 \pm 0.1A$	$1.25 \pm 0.5A$	$0.57 \pm 0.1A$	$1.26 \pm 0.4A$	$0.07 \pm 0.0A$
	EC	ш	$2.32 \pm 0.4b$	$12.53 \pm 1.4a$	$5.05 \pm 0.4a$	$0.072 \pm 0.012b$	$213 \pm 23b$	$0.44 \pm 0.0a$	$0.92 \pm 0.3ab$	$0.82 \pm 0.2a$	$19.00 \pm 7.0a$	$0.73 \pm 0.2a$
		뿔	$2.19 \pm 0.4A$	$9.51 \pm 1.3A$	$4.68 \pm 0.4AB$	0.068 ± 0.015 AB	$222 \pm 22B$	$0.45 \pm 0.0A$	$1.12 \pm 0.3A$	$0.81 \pm 0.2A$	$0.65 \pm 0.1A$	$0.04 \pm 0.0A$
	PS	끧	$0.73 \pm 0.1c$	$5.64 \pm 0.6b$	$7.34 \pm 0.3b$	$0.021 \pm 0.002c$	$119 \pm 6a$	$0.24 \pm 0.0b$	$0.15 \pm 0.0b$	$0.83 \pm 0.1a$	$34.45 \pm 5.1b$	$3.16 \pm 0.6b$
		岁	$0.71 \pm 0.1B$	$4.51 \pm 0.6B$	$6.22 \pm 0.5BC$	$0.021 \pm 0.002BC$	$147 \pm 26A$	$0.30 \pm 0.1B$	$0.26 \pm 0.0A$	$1.03 \pm 0.2A$	$1.28 \pm 0.4A$	$0.14 \pm 0.0B$
	CS	끧	$0.69 \pm 0.2c$	$4.85 \pm 1.3b$	$7.46 \pm 0.7b$	$0.020 \pm 0.007c$	$132 \pm 9a$	$0.25 \pm 0.0b$	$0.22 \pm 0.0b$	$0.68 \pm 0.2a$	$26.08 \pm 1.4ab$	$3.47 \pm 1.1b$
		뿔	$0.48 \pm 0.1B$	$3.38 \pm 1.1B$	$6.76 \pm 0.2C$	$0.014 \pm 0.004C$	$117 \pm 9A$	$0.23 \pm 0.0B$	$0.25 \pm 0.1A$	$0.70 \pm 0.1A$	$0.74 \pm 0.2A$	$0.13 \pm 0.0B$
R3	AC	ш	$2.32 \pm 0.3a$	$9.15 \pm 1.5a$	$4.07 \pm 0.3a$	$0.071 \pm 0.008a$	$148 \pm 17a$	$0.44 \pm 0.0a$	$0.35 \pm 0.1a$	$0.75 \pm 0.1a$	$25.51 \pm 4.3a$	$1.40 \pm 0.1a$
		뿔	$1.73 \pm 0.2A$	$6.94 \pm 0.5A$	$4.11 \pm 0.3A$	$0.052 \pm 0.005A$	$145 \pm 14A$	$0.42 \pm 0.0A$	$0.40 \pm 0.1A$	$0.54 \pm 0.1A$	0.88 ± 0.34	0.06 ± 0.0
	EC	ш	$2.62 \pm 0.6a$	$12.92 \pm 2.2ab$	$4.69 \pm 0.5a$	$0.083 \pm 0.020a$	$231 \pm 24b$	$0.51 \pm 0.0a$	$0.87 \pm 0.2a$	1.15 ± 0.1 ab	$16.66 \pm 3.4a$	$0.64 \pm 0.1a$
		뿔	$1.91 \pm 0.2A$	9.60 ± 0.6 AB	$4.75 \pm 0.3A$	$0.058 \pm 0.006A$	$226 \pm 18B$	$0.48 \pm 0.0A$	$0.81 \pm 0.1AB$	$0.85 \pm 0.1AB$	$0.66 \pm 0.2A$	ΗI
	S	ш	$2.62 \pm 0.3a$	$14.47 \pm 1.3b$	$5.50 \pm 0.4a$	$0.081 \pm 0.011a$	$189 \pm 23a$	$0.41 \pm 0.0a$	$1.28 \pm 0.1a$	0.99 ± 0.1 ab	$26.47 \pm 3.5a$	$0.97 \pm 0.2a$
		岁	$2.16 \pm 0.3A$	$12.20 \pm 0.4B$	$5.31 \pm 0.4A$	$0.074 \pm 0.008A$	$197 \pm 20AB$	$0.44 \pm 0.0A$	$1.59 \pm 0.0BC$	$1.40 \pm 0.2B$	$1.05 \pm 0.2A$	$0.04 \pm 0.0A$
	CS	ш	$3.45 \pm 0.6a$	$15.83 \pm 1.7b$	$5.10 \pm 0.4a$	$0.113 \pm 0.022a$	$211 \pm 21a$	$0.47 \pm 0.0a$	$2.60 \pm 0.4b$	$1.44 \pm 0.1b$	$24.29 \pm 2.4a$	$0.79 \pm 0.1a$
		Z	$2.51 \pm 0.4A$	$11.55 \pm 1.0AB$	$4.76 \pm 0.3A$	$0.078 \pm 0.014A$	$227 \pm 17B$	$0.49 \pm 0.0A$	$1.90 \pm 0.3C$	$1.40 \pm 0.1B$	$0.59 \pm 0.1A$	$0.03 \pm 0.0A$

Figure 4. Plant water status. The effect of four scenarios on the RWC and midday stem water potential (Ψ_{md}) in IE (black symbols) and NE (red symbols) poplars is shown. A, The measurement of RWC was performed on leaves 4, 8, and 12 (counting from the apex) based on nearinfrared reflectance. Values represent means of $n = 4 \pm sE$; dashed lines indicate the reference value of 80% RWC. Highlighted areas represent the periods of drought and heat. B, The Ψ_{md} measurements were performed during the last day of the third stress cycle in the PS scenario (S3) and after 7 d of recovery (R3). Values represent means of $n = 4 \pm se$; dashed lines indicate $\Psi_{md} = -1.0$ MPa. n/d, No data. The PS and CS scenarios were performed under elevated [CO₂].



severe water stress in CS (Fig. 4B). The final recovery phase in both stress scenarios showed no difference in the RWC or midday water potential between IE and NE poplars.

To understand the impact of HDSs on the leaf development of the IE and NE genotypes, we assessed the relative leaf expansion rate (RLER), leaf cell number, and cell size. The RLER reflects the increasing total LA during the HDS. We observed a strong reduction of RLER, similar in both genotypes, during PS and CS (50% and 56%, respectively), compared with that of enhanced [CO₂] only (both P < 0.001; data not shown). The strong positive correlation between the leaf-level MeOH emission rates at time point S3 (Fig. 3) and the RLER ($r^2 = 0.76$, P < 0.001; Fig. 5A) clearly indicates the suitability of the MeOH emissions as a marker of plant cell growth.

Overall, in the span of PS or CS (day 1–day 22), both genotypes developed fewer leaves than did the controls

(leaves per plant: 16, nine, and eight in ambient $[CO_2]$, PS, and CS, respectively; P < 0.001; data not shown). Moreover, the leaf dimensions of trees that were exposed to periodic and chronic stress were smaller than were those of the control plants (P = 0.002, both; Fig. 5C), with no difference between PS and CS (Fig. 5C). These changes in the leaf dimensions coincide with a positive correlation between the size of the leaf blade area and the number of adaxial epidermal cells in ambient $[CO_2]$ ($r^2 = 0.62$, P < 0.001), PS ($r^2 = 0.63$, P <0.001), and CS ($r^2 = 0.80$, P < 0.001; Fig. 5B). Apparently, the leaves that were grown in different scenarios exhibited the same developmental program (i.e. the leaves of a specific size grown in different climates have a comparable number of cells; Fig. 5D). Thus, the difference in the leaf size must be attributed to a significant reduction in the cell area under stress, as observed (Fig. 5E; P < 0.001 for both scenarios).

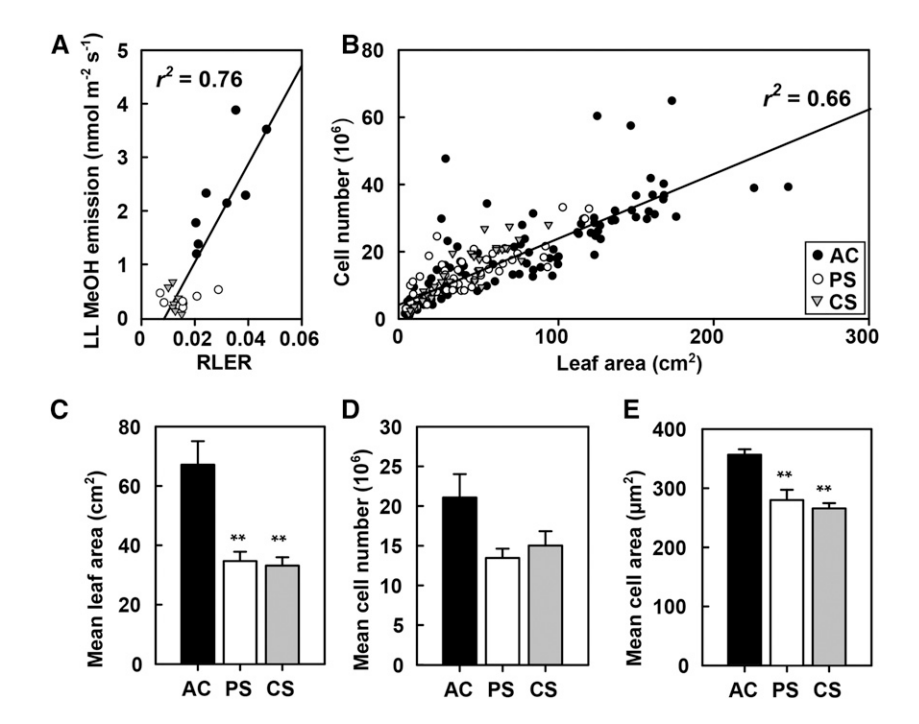


Figure 5. The effect of climate scenarios on the RLER, mean area per leaf, leaf cell number, and cell area. A, The relationship between leaf-level (LL) MeOH emission and the RLER in the AC (black circles), PS (white circles), and CS (gray triangles) scenarios. IE and NE poplar plants were combined within each scenario. The linear regression line was generated using the values at stress time point S3: y = 90.227x - 0.6703, $r^2 =$ 0.76, P < 0.001. B, The correlation of the LA with the corresponding cell number of leaves developed during HDSs (time point P until S3) in the scenarios AC, PS, and CS. The linear regression line is shown: y = 185,630.591x + 6,045,519.819, $r^2 = 0.66$, P < 0.001. C to E, Measurements of mean area per leaf (C), mean cell number (D), and mean cell area of leaves (E) that developed during stress. Values represent means of $n = 4 \pm \text{se}$. Significant differences between control (AC) and stress scenarios (PS and CS) are indicated: **, P < 0.001, ANOVA, LSD test. The PS and CS scenarios were performed under elevated [CO₂].

Enclosed Leaf-Level Measurements of Photosynthetic Parameters and Isoprene Emission

To compare plant-level (Figs. 2 and 3) with leaf-level measurements, we analyzed the photosynthetic gas exchange and VOC emission rates at the leaf scale under steady-state standard conditions (i.e. 30°C leaf temperature and $1,000~\mu\text{mol}$ photons m $^{-2}$ s $^{-1}$) at the time of maximum stress (S3) and after 7 d of final recovery (R3; Table I). At S3, the isoprene emission of fully developed IE leaves was 10% (35 nmol m $^{-2}$ s $^{-1}$) higher in PS and 15% (26 nmol m $^{-2}$ s $^{-1}$) lower in CS compared with that of the leaves of the ambient [CO $_2$] scenario (31 nmol m $^{-2}$ s $^{-1}$). The lowest isoprene emission rate was observed under elevated [CO $_2$] (up to 40% decrease compared with ambient [CO $_2$]). In general, the stimulating effect of HDSs on isoprene emission was less pronounced at the leaf scale compared with the plant scale (Fig. 3; Table I).

At S3, the *A* of the leaves that were exposed to HDSs decreased by approximately 55% in PS and 60% in CS (P < 0.001, both) compared with that of the control scenario under ambient $[CO_2]$. In accordance, the g_s , E and E_d , c_i , and, consequently, the ratio of intracellular to extracellular [CO₂] decreased during stress. The instantaneous WUE at the leaf level, calculated as the ratio of A over E, increased under elevated $[CO_2]$ (P = 0.033) and was greatest under stress scenarios (time point S3; P < 0.001, all). As expected, the plants that were grown under high [CO₂] generally exhibited a lower g_s and E than did the plants that were grown under ambient $[CO_2]$ (P < 0.001). For the plants that were grown under ambient $[CO_2]$, the A and g_s were higher in the IE genotype than in the NE genotype at S3 (P = 0.05) but not 1 week later (R3; P = 0.22). In general, the combination of temperature increase (+6°C, daily maximum) and water limitation had minor effects on the basal isoprene emission capacity while photosynthesis was impaired. As a consequence, the fraction of C that was emitted as isoprene (expressed on the basis of photosynthetic assimilated C) increased during HDSs, being highest under CS conditions in the IE genotype (3.5%), whereas it was negligible in the NE plants (less than 0.2%).

After 7 d of recovery (R3), the leaves from the trees that were grown under the PS and CS scenarios reached the same g_s , E, E_d , c_i , ratio of intracellular to extracellular [CO₂], and WUE as those of the leaves of the untreated control plants ([EC]), whereas the A exceeded that of the control level (PS, +15%; CS, +20%). Overall, the leaves from the IE genotypes had higher A rates (P < 0.001) in every scenario compared with NE plants.

Net C Uptake and Pigmentation

Based on the continuous reading of the plant net CO_2 (NEE) and net isoprene exchange fluxes throughout the experimental period, we calculated the net C uptake in each scenario based on the projected LA (NEE minus net isoprene exchange; Fig. 6). Overall, there was no significant difference between the poplar genotypes within each scenario. At the end of the experiment, the net C uptake under elevated $[CO_2]$ was approximately 22% higher in IE plants and 7% higher in NE plants compared with the ambient $[CO_2]$ control scenario. The PS scenario reduced the uptake of C by approximately 20% and 23% in IE and NE plants, respectively, compared with that under enhanced $[CO_2]$. In the CS scenario, the plants fixed less C than in PS (IE plants, -33%; NE plants,

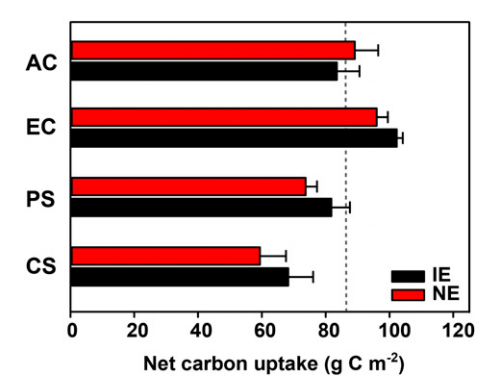


Figure 6. Net C uptake in IE (black bars) and NE (red bars) poplars in the four scenarios (AC, EC, PS, and CS) at the end of the experiment. Net C uptake was calculated based on overall plant fluxes of CO_2 and isoprene (see "Materials and Methods"), and values for IE and NE plants in each scenario are given as means of four subchambers \pm se. The dashed line indicates the reference value of 87 g C m⁻² (the mean in the AC scenario for IE plants). The PS and CS scenarios were performed under elevated [CO₂].

-38%). Concurrent with the reduction of net C uptake, the amount of C lost as isoprene increased in the IE plants by 6 to 9 times during the periodic or chronic HDSs compared with control conditions. The percentage of photosynthetic C lost as isoprene (daily) increased progressively as the water scarcity became more severe (Supplemental Fig. S6), finally reaching 5.8% at day 20 in the CS scenario.

As an additional measure of leaf performance under abiotic stress, we noninvasively monitored the anthocyanin, flavonol, and chlorophyll contents in the leaves using an optical sensor. Cultivation under high [CO₂] resulted in higher contents of anthocyanins and flavonoids in both of the genotypes compared with cultivation under ambient $[CO_2]$ (P < 0.001; Supplemental Fig. S7). The application of HDSs reduced the anthocyanin and flavonoid contents in the leaves that were grown under CS (P < 0.001 and P = 0.01, respectively) but not in PS (P = 0.34 and P = 0.49, respectively) compared with the enhanced [CO₂] control. The chlorophyll content in the leaves remained unchanged throughout the experiment within the four scenarios. However, under ambient [CO₂], the NE leaves had lower chlorophyll contents than that in the IE plants (P < 0.05).

DISCUSSION

Online Analysis at the Plant Level Displays the High Fluctuation of Gas Exchange and VOC Emissions under the Different Climate Scenarios

While many studies have investigated leaf-level measurements of photosynthetic processes, transpiration, and isoprene emission, most of these studies have only reported measurements from a single point in time and from one distinct leaf. In contrast, online measurements at the canopy (plant) scale provide a dynamic,

intrinsic view of the overall plant behavior under changing environmental conditions, herein climate scenarios, considering whole-ecosystem processes (such as microclimatic factors inside a canopy; Zhu et al., 2012) and allowing direct measurements of net CO₂ and VOC fluxes from entire plants. The interaction between rising temperatures, elevated [CO₂], and drought stress (during HDSs) led to a strong increase in constitutive isoprene emission. This effect was less pronounced when analyzing the standard emission factor at the leaf level (1.5 times higher than in ambient [CO₂]), while the overall plant response was much stronger (9 times higher expressed based on the LA, 7 times higher expressed per plant). This increase in the overall plant isoprene fluxes is most likely a combination of the temperature and drought on isoprene emission. At the plant scale, the measured air temperature (33°C) and leaf temperature (33°C–37°C; Supplemental Fig. S4) during HDSs were higher than at the leaf level (30°C, leaf temperature). As temperature is the main driver of ISOPRENE SYNTHASE (ISPS) enzyme activity, the strong increase in the isoprene emission during HDSs is probably a combined function of enhanced ISPS activity and higher substrate availability (Rasulov et al., 2010). Drought can also promote isoprene emission, albeit with a concomitant decrease in photosynthesis (Monson et al., 2007; Tattini et al., 2014), probably as a result of decreased c_i (Table I). The ascent in canopy isoprene emission over time in the PS and CS scenarios reflects long-term acclimation to high temperatures. Here, gene activation may lead to higher ISPS amounts (Wiberley et al., 2005). Fortunati et al. (2008) showed in a combined temperature and drought experiment a decrease in leaf isoprene emission when drought was prolonged. There, the decrease in the isoprene emission was in concert with the mRNA transcript level, the protein amount, and the ISPS activity and could not be offset by the elevated temperature (35°C instead of 25°C).

The reductions in isoprene emission capacity and overall plant emission at elevated $[CO_2]$ are consistent with previous studies on different *Populus* spp. (e.g. *Populus deltoides* in Rosenstiel et al. [2003], *Populus* × *euroamericana* in Centritto et al. [2004], *P. deltoides* and *Populus tremuloides* in Wilkinson et al. [2009], and $P. \times canescens$ in Way et al. [2011]). However, the repressive effect of elevated $[CO_2]$ on the isoprene emission herein was more moderate, probably due to the lower experimental increase of $[CO_2]$ (500 μ L L⁻¹) compared with the aforementioned studies or the high degree of species-specific variability (*Populus alba* in Loreto et al. [2007]), with some poplar genotypes even not showing any reduction (Eller et al., 2012).

Poplars Pay for Stress Adaption by Significant Reductions in C Gain

In the context of plant stress concepts (Lichtenthaler, 1996), the present climate change simulations effectively demonstrate plant stress resistance strategies: in other words, the ability of Grey poplar to tolerate unfavorable

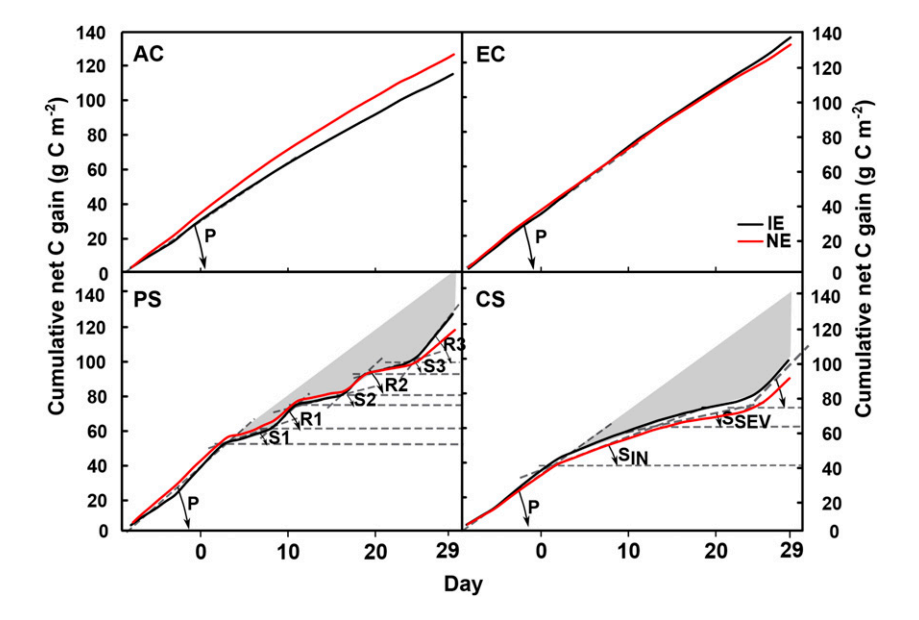


Figure 7. Cumulative net C gain in IE (black lines) and NE (red lines) Grey poplar in the four scenarios (AC, EC, PS, and CS). Dashed lines represent auxiliary lines to calculate the angles between the x axis and the linear slope of each indicated phase. Different phases are indicated as exemplary for IE poplars. In the CS scenario, the phases are named as follows: P, prestress; S_{IN} , stress initial; S_{SEV} stress severe; and R, recovery. The gray areas illustrate the C that the plants were not able to gain due to stress incidence.

conditions (Levitt, 1980) and adapt to them. The photosynthetic performance in the PS and CS scenarios shows features of eustress, which is per definition a mild, stimulating stress, strengthening plant resistance (Lichtenthaler, 1996). In this study, the NEE of poplar temporarily deviated from the normal physiological standard without exceeding the plant's limit of tolerance (i.e. its resistance minimum; Lichtenthaler, 1996), leading to irreversible damage, as demonstrated by the fast and complete reversibility of the response, suggesting that the integrity of the photosynthetic machinery was maintained during HDSs, another characteristic of drought resistance (Sofo et al., 2004; Gallé and Feller, 2007). Therefore, stomatal constraints were likely the main factors responsible for the decrease in NEE, as observed when water stress is moderate (Chaves et al., 2003), as in the PS and CS scenarios.

During recovery from HDSs (short-term recoveries in PS and long-term recovery in PS and CS) the net C gain of both poplar genotypes returned to higher rates than the prestress and control values (AC and EC [angle (R3) > angle(P)]; Fig. 7; Supplemental Table S2). Here, the experience of HDSs stimulated cell metabolism and established a new physiological optimum with a higher daily NEE. Such an overcompensation of the *A* during rewatering after drought stress has been reported several times (Correia et al., 2014). However, how long the priming effect in the Grey poplar plants is maintained remains to be elucidated.

We could not detect any inducible C6 volatiles that were produced from polyunsaturated fatty acids (LOX products; Feussner and Wasternack, 2002) throughout the experiment. LOX products are reliable stress markers of oxidative stress and indicate membrane damage (Beauchamp et al., 2005; Loreto et al., 2006). Thus, this result suggests that the threshold for oxidative membrane damage in Grey poplar was not exceeded during and after the stress events, and the emission

of LOX products may not be a reliable feature of drought stress in poplar. The rapid and transient emission of LOX products has been reported in response to other abiotic factors, including high temperature (Behnke et al., 2013), flooding (Copolovici and Niinemets, 2010), and ozone (Beauchamp et al., 2005), as well as biotic stimuli (Ghirardo et al., 2012). However, LOX emissions upon dehydration have been detected as early stress responses on cut grass (de Gouw et al., 1999; Brilli et al., 2012). These drought treatments were, in contrast to our climate change scenarios, rather extreme and artificial and resulted in fast dehydration that normally does not occur in natural drought progression. It was proposed that, under oxidative stress, a substantial fraction of isoprene is oxidized inside the leaf to MVK and/or MACR (Jardine et al., 2012). Here, we could not detect any isoprene oxidation products in measurements at the plant level (with a proton-transfer reaction-quadrupole mass spectrometer [PTR-QMS]) or at the leaf level (with a protontransfer reaction-time of flight-mass spectrometer [PTR-ToF-MS]).

While HDSs positively triggered isoprene emission rates and NEE, we observed a long-lasting impairment of plant growth and leaf pigmentation (anthocyanins and flavonols) in both IE and NE plants during HDSs and during the recovery phases. The strong correlation between MeOH emission and RLER clearly demonstrates that MeOH is a suitable indicator of overall plant growth. The phylogenic emission of MeOH is primarily associated with leaf expansion and cell elongation (Nemecek-Marshall et al., 1995; Fall and Benson, 1996; Hüve et al., 2007), and developing poplar leaves emit significantly more compared with mature ones (Ghirardo et al., 2011). The recovery of NEE in contrast to plant growth demonstrates that water limitation exerted a greater impact on cell growth (site of C use and sink activity) than on photosynthetic processes (site

of C gain and source activity). It is common in many plant species that are exposed to moderate drought that C use (growth) decreases before the C source (photosynthesis) is impaired (Hummel et al., 2010). When stress limits resources, plants must balance primary and secondary metabolism, investing in either plant growth or protective strategies. We did not observe an accumulation of polyphenols (anthocyanins and flavonols) in the leaves of either the IE or NE genotype under stress exposure. However, the pool of polyphenols increased under elevated $[CO_2]$ compared with ambient $[CO_2]$ conditions (Supplemental Fig. S7), as reported previously (Kuokkanen et al., 2001).

Isoprene Emission Is Not Essential for Poplar to Adapt to Fast-Changing Environmental Extremes

In addition to the general physiological performance of Grey poplar under predicted future short-term extremes, we also aimed to quantify the environmental impact on transgenic poplar genotypes with an almost complete absence of isoprene emission (Behnke et al., 2007, 2010a). This interest is motivated by the proposed function of isoprene in plant stress mitigation (Loreto and Schnitzler, 2010) and the potential for biotechnological generation or the phenotyping of low-isopreneemitting or NE poplars as a strategy to minimize the harmful effects of large poplar plantations on local air quality and human health (Ainsworth et al., 2012; Rosenkranz et al., 2014). The latter issue is especially important because the pollution of the atmosphere by isoprene is predicted to increase due to the promotion of new poplar plantations worldwide (IPC, 2008).

Globally, the IE and NE genotypes performed similarly under the different stress scenarios, indicating that the absence of isoprene emission marginally influences physiology, even under PS and CS exposure. This result is in accordance with an earlier observation in which comparable growth rates, biomass yield, and (projected) CO₂ uptake were reported in IE and NE plants grown for two vegetation periods under seminatural conditions (Behnke et al., 2012). The authors presumed that the absence of any climate extreme in their field trail might mask different sensitivities to abiotic stress and proposed experiments under more harsh environmental conditions to prove the potential stressalleviating function of isoprene. Here, after HDSs, we observed similar growth performance in both genotypes (Fig. 5). That IE plants somehow must pay for the release of C as isoprene was recently reported for transgenic IE tobacco (Nicotiana tabacum; Ryan et al., 2014). These authors showed that drought stress resulted in slower growth of IE plants relative to the NE wild-type or vector control plants. In the control scenarios, we observed a lower cumulative net C gain in IE plants under ambient [CO₂] (Fig. 7). This difference, however, vanished under elevated [CO₂] conditions, concomitant with decreases in the metabolic differences between IE and NE plants (Way et al., 2013), possibly due to the inhibitory effect of elevated $[CO_2]$ on the methylerythritol 4-phosphate pathway flux (Ghirardo et al., 2014) and isoprene biosynthesis (Rosenstiel et al., 2003; Possell and Hewitt, 2011).

The strongest difference that was observed between the genotypes was an impaired ETR in the NE plants during each stress cycle (Fig. 2; PS) and when stress progressed (Fig. 2; CS). In contrast, the ETR in IE plants remained stable or became even slightly increased, possibly due to increased leaf temperatures during HDSs (Copolovici et al., 2005; Behnke et al., 2007). Different tolerance of ETR in IE and NE Grey poplar upon abiotic (heat and light) stress has been reported previously (Behnke et al., 2010b; Way et al., 2011). ETR reflects the quantum yield of PSII and provides information about the light reaction of photosynthesis and CO₂ assimilation (Genty et al., 1990). Because ETR is thylakoid membrane localized, reduced ETR in heatstressed NE plants may be explained as a consequence of altered membrane stability (Singsaas et al., 1997; Velikova et al., 2011) and/or of direct interaction of isoprene with reactive oxygen species, resulting in lower oxidative damage and lipid peroxidation (Loreto and Velikova, 2001; Velikova et al., 2005; Vickers et al., 2009). Recent findings by Velikova et al. (2014, 2015) suggest that the lower ETR in NE plants may result from subcellular remodeling processes that occur in NE chloroplasts, possibly as a consequence of the RNA interference-mediated silencing of the ISPS. The analysis of the chloroplast ultrastructure, the proteome, and the lipid composition of the thylakoid membrane of IE and NE poplars (Velikova et al., 2014, 2015) revealed a comprehensive structural and functional reorganization in the thylakoid membranes of NE plants. The lower amount of unsaturated fatty acids (i.e. linolenic acid) associated with a lower abundance of two oxygen-evolving complexes, PsbP, and PsbQ (subunits of PSII), and of the cytochrome $b_6 f$ complex may affect the electron flow under stress conditions. During drought and heat, when the photoinhibition of PSII often occurs (Murata et al., 2007), the reduced basic equipment of components of the electron transport chain in NE plants may be insufficient to maintain the same ETR as isoprene-emitting plants. Furthermore, in NE plants, several components of the PSII repair cycle are down-regulated (thylakoid formation protein and thylakoid lumen protein 18.3; Velikova et al., 2014), further promoting photoinhibition, as the extent of photoinhibition depends strongly on the plant's ability to repair PSII (Takahashi and Murata, 2008).

Despite these differences in the biochemical and biophysical properties, NE plants are not deterred in growth or CO₂ fixation in a future, high-[CO₂] climate with recurring HDSs. Moreover, a recent phytotron study demonstrated that long-term cultivation (9 months) under enhanced [CO₂] diminishes the physiological and metabolic differences between IE and NE plants (Way et al., 2011, 2013), indicating that the beneficial function of isoprene emission via the enhanced abiotic stress tolerance of photosynthetic processes

(Loreto and Schnitzler, 2010) under future climate conditions might be of lesser importance.

CONCLUSION

Overall, we aimed to quantify the dynamics of the superposed effects of three global change factors (temperature, [CO₂], and water limitation) on the photosynthetic performance, VOC emissions, leaf growth, and C uptake by the woody model species Grey poplar.

The use of highly controlled phytotron chambers allowed us to enclose the whole canopy of small Grey poplar trees to simultaneously measure single-leaf and whole-plant responses to the periodic and chronic heat and drought events that were predicted in the future climate (IPCC, 2014). The data clearly showed that whole-plant isoprene fluxes increased dynamically and strongly under the HDSs, although the plants developed fewer and smaller leaves under these conditions. The poplars were able to tolerate PS and CS events but paid for their stress adaption with temporarily reduced A and C gain. However, the higher photosynthesis rates at the end of the recovery phase suggest that the impact of periodic and chronic HDSs on growth and biomass can be compensated under unstressed conditions in due time. The comparison of photosynthesis, growth, and stress parameters in the IE and NE poplars suggests that isoprene emission does not enhance plant stress mitigation under the future climate in poplar.

MATERIALS AND METHODS

Plant Material and Growth Conditions

The experiments were conducted with four genotypes of Grey poplar (Populus × canescens [INRA clone 7171-B4]; syn. Populus tremula × Populus alba). Two IE genotypes (wild type and PcISPS:GUS/GFP, in which the PcISPS promoter was fused to the GUS and GFP reporter genes; for details, see Cinege et al., 2009) and two wellcharacterized NE transgenic genotypes (35S::PcISPS-RNAi lines RA1 and RA2; Behnke et al., 2007; Way et al., 2013) were used. Plantlets were amplified by micropropagation under sterile conditions (Leplé et al., 1992), and rooted plantlets (approximate plant height of 5 cm) were cultivated in the greenhouse in 2.2-L pots on a sandy soil (1:1 [v/v] silica sand and Fruhstorfer Einheitserde). For optimum fertilization, the soil was initially mixed with a mixture of slow-release fertilizers (Triabon [Compo] and Osmocote [Scotts Miracle-Gro]; 1:1, 10 g L⁻¹ soil). Furthermore, we applied a liquid fertilizer every 2 weeks for the duration of the experiment (0.1% $\left[w/v\right]$ Hakaphos Grün; Compo). Climate conditions in the greenhouse were maintained at a 16/8-h photoperiod with supplemental lighting (200-240 μ mol photons $\mathrm{m}^{-2}~\mathrm{s}^{-1}$ at the canopy level, photosynthetically active radiation [PAR]). The temperature was set to 22° C/ 18° C (day/night), and [CO₂] was ambient (380 μ L L⁻¹). The plantlets were raised for 5 weeks in the greenhouse before they were moved to the phytotron chambers for the next 7.5 weeks into different climatic scenarios and [CO₃] (see below). When the plants were placed into the phytotron chambers, they had reached a height of 40 ± 5 cm and leaf number of 12 ± 2 . Before starting the stress scenarios (PS and CS), the plants were cultivated for 25 d to adapt growth and physiology under ambient and enhanced [CO₂] control conditions (AC and EC). At the start of first HDS, the plants were 8.5 weeks old. At the end of the experiment (after 52 d in the phytotron chambers), the plant height was 125 \pm 7 cm in the control scenarios (AC and EC) and 111 \pm 7 cm in the stress scenarios (PS and CS). The leaf number was 39 \pm 5 in the AC and EC scenarios and 31 \pm 4 in the PS and CS scenarios.

Climate Change Scenarios

The simulation of the different environmental conditions was performed in four walk-in-size phytotron chambers at the Helmholtz Zentrum München (for

details, see Seckmeyer and Payer, 1993). Each phytotron chamber contained four subchambers made of acrylic glass (about 1 m³ in volume). In each subchamber, one genotype (wild type, GUS/GFP, RA1, or RA2; 12 plants from each) was accommodated. Each subchamber was equipped with combined air temperature and relative humidity sensors and were flushed (40 m³ h $^{-1}$) by purified air (charcoal filtered) adjusted in temperature, humidity, and [CO $_2$]. To achieve irradiation regimes very close to solar outdoor conditions from UV light to the near-infrared light, the phytotron facility uses a combination of different lamps and filters that enables the simulation of the daily course of solar radiation from sunrise to sunset (Thiel et al., 1996). Details of climate conditions and plant arrangement in the subchambers are shown in Supplemental Figure S1.

We simulated four environmental scenarios, with the first two (1 and 2) as present and future controls (daily maximum temperature of 27°C, no stress episodes) and two stress scenarios (3 and 4) with periodic and chronic exposure of increased temperatures (control temperature + 6° C, daily maximum temperature of 33°C) and water limitation (see below). The scenarios are as follows (Fig. 1). (1) AC: control with ambient [CO $_2$] = 380 $\mu L~L^{-1}$. (2) EC: control with elevated $[CO_2] = 500 \,\mu\text{L L}^{-1}$. (3) PS: PS containing three cycles (each 6 d) with increased temperature and concomitant, acute drought (hereafter referred to as HDSs). Between the first and second and the second and third HDSs, a recovery time of 2 d was implemented, where temperature declined to the control level (27°C) and plants were irrigated to pot capacity. (4) CS: CS with slowly developing drought progressing over 22 d from day 0 to day 22 (during these days, temperature was increased as in PS). The HDSs in the PS and CS scenarios are followed by a final recovery time of 7 d (from day 22 to day 29) where temperature decreased to the control level and pots were irrigated to saturation. The [CO₂] in the PS and CS scenarios was elevated as in EC (500 μ L CO₂ L⁻¹). The CO₂ concentrations in all scenarios followed naturally occurring diurnal variations. The elevated CO₂ environment in the EC, PS, and CS scenarios was created by the injection of pure CO₂ (120 μ L L⁻¹) into the air stream of the ambient [CO₂]. In our analysis, the AC scenario is the direct control of the PS and CS scenarios, while the EC scenario was used to compare the reported inhibitory effect of elevated [CO₂] on leaf-level isoprene emission (Wilkinson et al., 2009; Way et al., 2011) with canopy-scale dynamics (Sun et al., 2013). There was no attempt to separate temperature and drought factors in this study.

The experiment was repeated twice with exchanging the scenarios between the phytotron chambers and the position of each genotype in the subchambers to avoid position effects. Genotypes were pooled according to their isoprene emission capabilities: wild-type and GUS/GFP genotypes to isoprene-emitters and RA1 and RA2 to nonemitters. The start of the first HDS (PS) and the beginning of the progressive drought (CS) is termed as day 1 of the experiment; at this time point, IE and NE plants exhibited a mean height \pm se of 74 ± 4 cm and 72 ± 3 cm, respectively. Also, the mean number of leaves did not differ between IE and NE plants (IE plants, 28 ± 0.4 ; NE plants, 28 ± 1).

Plant Irrigation and Simulation of Water Scarcity

The controlled water regime was obtained using automated drip irrigation systems placed in each pot halfway between the stem and the edge of the pot. Plants were exposed to short-term (in PS) and long-term (in CS) drought by reducing the amount of irrigation water gradually during each HDS (Supplemental Fig. S1C). In the PS scenario, three drought cycles were imposed to mimic natural wet/dry cycles in the field. In the first, second, and third cycles, the amount of water was reduced by 50%, 60%, and 70%, respectively, compared with AC and EC. To slow the progression of drought in the CS scenario, in the first 5 d the irrigation amount was reduced by only 30% compared with fully watered controls in AC and EC. Every 5 d, the water amount in CS was reduced by 10%, reaching a reduction of 70% compared with the controls.

Sampling Protocol and Measurements

On a weekly basis, we monitored noninvasively the leaf relative water content, leaf temperature, chlorophyll fluorescence of PSII, and leaf pigmentation. Measurements were performed on six random plants of each scenario and genotype at five to seven time points throughout the experiment, reflecting physiologically important time points of the PS scenario: prestress (P), stress 1 (S1), recovery 1 (R1), stress 2 (S2), recovery 2 (R2), stress 3 (S3), and recovery 3 (R3; Fig. 7). Measurements were performed directly in the subchambers and always between 10 AM and 2 PM Central European Time, when irradiation and chamber air temperature were at their maxima.

Overall plant-level gas exchange and VOC measurements were performed online with an hourly resolution from inlet and outlet air of the subchambers.

Moreover, we measured both parameters at the leaf level under constant conditions at the time points S3 and R3 (see below). Destructive samplings were taken at the maximum stress (S3) and after the final recovery (R3).

Overall Plant LA Estimation

The daily canopy LA was estimated from the total number of leaves, plant height (both assessed twice per week), and LA obtained from photographs taken on three reference plants per genotype and scenario at time points P and S3. The number of leaves lost during the experiment (aging) was taken into account. At the two destructive samplings (S3 and R3), the area of all leaves was measured (approximately 25), except the upper leaves harvested for biochemical and molecular biological analyses. The overall LA of 12 plants (six plants during R3) was used to calculate gas exchange and VOC emission fluxes at the plant level.

Growth Analysis of Leaves

For growth analysis of leaves, photographs and leaf discs of three plants per genotype and scenario were taken before (P) and after (S3) the stress treatments. Photographs were used to calculate RLER from the formula RLER = $\ln(\text{LA}_{\text{S3}}) - \ln(\text{LA}_{\text{P}})/\Delta t$, where LA is total LA before (P) or after (S3) the stress treatment and Δt is the duration of the HDSs (22 d). LAs were calculated for each individual plant using photographs from each leaf. For cell number and cell area analysis, small discs cut out from the middle part of each photographed leaf were immediately placed in ethanol followed by lactic acid. Samples with high starch levels were cleared and mounted in Hoyer's solution on microscope slides (Wuyts et al., 2010). Microscopic images of the adaxial epidermal cells (approximately 30–40 cells) were used to draw cells (using Image] software), and from the drawings obtained the cell size and cell number were calculated (Andriankaja et al., 2012). These values, together with the respective LAs, were used to calculate the cell number in each leaf. For growth analysis, data were not available for the EC scenario.

Plant Water Status

To monitor the plant water status over time, leaf water content was measured noninvasively using the spectroradiometer HR-1024 (Spectra Vista). Reflectance (R) of the upper leaf surface was recorded from 350 to 2,500 nm using the leaf probe equipped with an internal tungsten halogen lamp illuminating either the reference plate (white disk of R > 99%) or the leaf upon a black disk (R < 5%). Two measurements were taken at leaf 4 and four measurements at leaves 8 and 12 (from the apex). From the R measurements, the MSI = R(1,600 nm)/R(820 nm) was calculated according to Hunt and Rock (1989) and linearly correlated to the RWC of the leaves. In order to calculate RWC, a drying experiment was performed: intact leaves were cut and transferred to sealed tubes containing water, allowing them to hydrate to a constant level overnight, defined as weight (W) at full turgor (W_{FT}). The next day, leaves were placed on a bench to desiccate. R spectra and W were measured every 30 min. Finally, leaf samples were oven dried at 90° C for 24 h to determine the dry weight (W_{DW}). RWC was calculated according to RWC = ($W - W_{DW}$)/($W_{FT} - W_{DW}$).

The water potential of the plants was determined at midday using Scholander pressure chambers (Scholander et al., 1965). Measurements of water potential at midday were performed only at time points S3 and R3 when destructive sampling was performed.

Online Plant-Level Gas Exchange and VOC Analysis

 $[CO_2]$ and [water] in the ambient air were measured with two infrared gas analyzers (one for two scenarios; Rosemount 100/4P [Heinz Walz]) continuously and sequentially throughout the entire experiment by switching to the outlet of each subchamber (four per scenario) every 5 min. Every 20 min, the inlet air of the chambers was measured. From the difference between the outlet and inlet $[CO_2]/[water]$ of each subchamber, the whole plant (canopy) NEE and evapotranspiration were calculated according to the equation of von Caemmerer and Farquhar (1981). These fluxes of CO_2 and water were then normalized to LA units using the canopy LA estimation of every given day (see above).

Online determination of isoprene (m69), MeOH (m33), m71, LOX products (m99 and m101), and monoterpenes and sesquiterpenes (m137 and m205, respectively) was conducted simultaneously to the gas-exchange measurements using a high-sensitivity PTR-QMS (Ionicon Analytik) at a sampling flow rate of 200 mL min⁻¹. The PTR-QMS switched between the two infrared gas analyzers every 2 d. The details of the PTR-QMS operating parameters and the calibration procedures are given elsewhere (Ghirardo et al., 2010; Kreuzwieser et al., 2014).

In addition, the sum of the isoprene oxidation products MVK and MACR was calculated at m71, after subtracting the amount of isoprene occurring as stable ^{13}C isotope (i.e. $^{13}\text{C}_2^{12}\text{C}_3\text{H}_8; 0.305\%$ of m69). The first 1 min of each measurement after switching the subchambers was always discarded in order to avoid any memory effects. VOC concentrations in the inlet air of the subchambers were used as background and therefore subtracted from the outlet concentrations every 20 min. In general, VOC emission rates were expressed per LA unit (m²); for isoprene, we also calculated the isoprene emission rate per plant.

Leaf-Level Gas-Exchange and VOC Analyses

Leaf-level gas exchange measurements were performed under constant light and temperature using two GFS-3000 instruments (Heinz Walz) with an 8-cm² clip-on-type cuvette connected online with a PTR-ToF-MS. The measurements were performed on attached leaves (no. 9 from the apex) under standard conditions (30°C, 1,000 μ mol photons m $^{-2}$ s $^{-1}$, and air humidity of 10,000 μ L L $^{-1}$). The cuvette was flushed with synthetic air with growth [CO $_2$] (AC, 380 μ L CO $_2$ L $^{-1}$; EC, PS, and CS, 500 μ L CO $_2$ L $^{-1}$). The measurements were carried out on time points S3 and R3 on four plants per genotype and scenario. Each measurement cycle took 40 min per plant and was split into three time ranges: 10 min of light in the cuvette, 20 min (25 min in the second experiment) of dark in the cuvette, and 10 min (5 min in the second experiment) of background of the empty cuvette (blank for the PTR-ToF-MS). While sampling from one cuvette, and was allowed to acclimatize for 40 min before the measurement cycle began.

A Teflon bypass (heated) was inserted at the cuvette outlet, and a PTR-ToF-MS (Graus et al., 2010) drew air from the back stream lines (Supplemental Fig. S1E). The PTR-ToF-MS was operated under standard conditions, 60°C drift-tube temperature, 540 V drift voltage, and 2.3 mbar drift pressure, corresponding to an E/N of 120 Townsend (E being the electric field strength and N the gas number density; 1 Townsend = 10^{-17} V cm²). The instrument was calibrated once per week by dynamic dilution of VOC using a gas standard (Apel Riemer Environmental). Full PTR-ToF-MS mass spectra were recorded up to m315 with a 1-s resolution time. Raw data analysis was performed using the routines and methods described by Müller et al. (2010).

PSII Fluorescence

Fluorescence was determined by a pulse modulation fluorometer (MiniPAM; Heinz Walz) for six plants per genotype and scenario. On the basis of the measured quantum yield and PAR, the ETR was calculated to according the following equation: yield \times PAR \times 0.5 \times 0.8, where 0.5 represents the fraction of light to PSII and 0.8 accounts for the leaf absorptivity (Genty et al., 1990).

Statistics

Each subchamber was treated as one biological replicate and contained plants of the same genotype (wild type, GUS/GFP, RA1, or RA2). Nondestructive measurements conducted on six plants per subchamber (four plants for leaf-level gas exchange) were first averaged to one measurement per subchamber, and the statistics were determined on the means of each subchamber. Mean values of $n=4\pm sE$ were calculated for isoprene emitters and nonemitters by pooling together the two repetitions of the experiment and the wild type with GUS/GFP (isoprene emitters) and RA1 with RA2 (nonemitters). ANOVAs were performed for each measurement time point (P, S1, R1, S2, R2, S3, and R3) using the two factors scenarios (AC, EC, PS, and CS) and genotypes (isoprene emitters and nonemitters). A posthoc test (with Bonferroni correction) followed the ANOVA to assess pairwise comparisons between particular scenarios and the poplar genotypes. Genotype effects were always tested between isoprene emitters and nonemitters.

Online gas-exchange and VOC emission data were tested based on integrated daily fluxes averaged over the above described measurement time points (P, S1, R1, S2, R2, S3, or R3). Pearson correlation tests were performed to identify relationships between RWC and MSI (Supplemental Fig. S5) and between MeOH emission (leaf level) and RLER (Fig. 3). In all cases, the results were considered significant at P < 0.05. All analyses were performed in SPSS version 22.0 (SPSS, Inc.).

Supplemental Data

The following supplemental materials are available.

Supplemental Figure S1. Time courses of air temperature, relative humidity, irrigation, and plant appearance in the four scenarios.

- **Supplemental Figure S2.** Representative day (day 20) showing the overall plant isoprene emission, MeOH emission, and NEE in the four scenarios.
- Supplemental Figure S3. Time course of m71 and LOX product (i.e. m99 + m101) emission rates of IE (black circles) and NE (red circles) Grey poplar genotypes in the four scenarios (AC, EC, PS, and CS).
- **Supplemental Figure S4.** Infrared thermography to measure leaf temperature of IE (black) and NE (red) Grey poplar in the four scenarios.
- Supplemental Figure S5. Drying experiment to assess the moisture stress index and the relative water context of Grey poplar leaves.
- **Supplemental Figure S6.** Time course showing the daily percentage of the photosynthetic C loss as isoprene in the four scenarios.
- Supplemental Figure S7. Effect of four scenarios on the anthocyanin index, flavonol index, nitrogen balance index, and chlorophyll index of IE (black circles) and NE (red circles) poplar genotypes.
- **Supplemental Table S1.** Results of two-way ANOVAs and Bonferroni posthoc tests for all measured parameters.
- Supplemental Table S2. Calculated angles of different stress phases of cumulative net C gain.

ACKNOWLEDGMENTS

We thank the phytotron staff of Helmholtz Zentrum München for helping to maintain the experiment and Violeta Velikova and Amy Trowbridge for constructive comments on the article.

Received June 9, 2015; accepted July 10, 2015; published July 10, 2015.

LITERATURE CITED

- Affek HP, Yakir D (2002) Protection by isoprene against singlet oxygen in leaves. Plant Physiol 129: 269–277
- Affek HP, Yakir D (2003) Natural abundance carbon isotope composition of isoprene reflects incomplete coupling between isoprene synthesis and photosynthetic carbon flow. Plant Physiol 131: 1727–1736
- Ainsworth EA, Yendrek CR, Sitch S, Collins WJ, Emberson LD (2012) The effects of tropospheric ozone on net primary productivity and implications for climate change. Annu Rev Plant Biol 63: 637–661
- Alemayehu FR, Frenck G, van der Linden L, Mikkelsen TN, Jorgensen RB (2014) Can barley (Hordeum vulgare L.) adapt to fast climate changes? A controlled selection experiment. Genet Resour Crop Evol 61: 151–161
- Allen SJ, Hall RL, Rosier PTW (1999) Transpiration by two poplar varieties grown as coppice for biomass production. Tree Physiol 19: 493–501
- Andriankaja M, Dhondt S, De Bodt S, Vanhaeren H, Coppens F, De Milde L, Mühlenbock P, Skirycz A, Gonzalez N, Beemster GT, et al (2012) Exit from proliferation during leaf development in *Arabidopsis thaliana*: a not-so-gradual process. Dev Cell 22: 64–78
- Arneth A, Schurgers G, Hickler T, Miller PA (2008) Effects of species composition, land surface cover, CO₂ concentration and climate on isoprene emissions from European forests. Plant Biol (Stuttg) 10: 150–162
- Ashworth K, Folberth G, Hewitt CN, Wild O (2012) Impacts of near-future cultivation of biofuel feedstocks on atmospheric composition and local air quality. Atmos Chem Phys 12: 919–939
- Aylott MJ, Casella E, Tubby I, Street NR, Smith P, Taylor G (2008) Yield and spatial supply of bioenergy poplar and willow short-rotation coppice in the UK. New Phytol 178: 358–370
- Bauwe H, Hagemann M, Fernie AR (2010) Photorespiration: players, partners and origin. Trends Plant Sci 15: 330–336
- Beauchamp J, Wisthaler A, Hansel A, Kleist E, Miebach M, Niinemets Ü, Schurr U, Wildt J (2005) Ozone induced emissions of biogenic VOC from tobacco: relationships between ozone uptake and emission of LOX products. Plant Cell Environ 28: 1334–1343
- Behnke K, Ehlting B, Teuber M, Bauerfeind M, Louis S, Hänsch R, Polle A, Bohlmann J, Schnitzler JP (2007) Transgenic, non-isoprene emitting poplars don't like it hot. Plant J 51: 485–499
- Behnke K, Ghirardo A, Janz D, Kanawati B, Esperschütz J, Zimmer I, Schmitt-Kopplin P, Niinemets Ü, Polle A, Schnitzler JP, et al (2013)

- Isoprene function in two contrasting poplars under salt and sunflecks. Tree Physiol 33: 562–578
- Behnke K, Grote R, Brüggemann N, Zimmer I, Zhou G, Elobeid M, Janz D, Polle A, Schnitzler JP (2012) Isoprene emission-free poplars: a chance to reduce the impact from poplar plantations on the atmosphere. New Phytol 194: 70–82
- Behnke K, Kaiser A, Zimmer I, Brüggemann N, Janz D, Polle A, Hampp R, Hänsch R, Popko J, Schmitt-Kopplin P, et al (2010a) RNAi-mediated suppression of isoprene emission in poplar transiently impacts phenolic metabolism under high temperature and high light intensities: a transcriptomic and metabolomic analysis. Plant Mol Biol 74: 61–75
- Behnke K, Loivamäki M, Zimmer I, Rennenberg H, Schnitzler JP, Louis S (2010b) Isoprene emission protects photosynthesis in sunfleck exposed Grey poplar. Photosynth Res 104: 5–17
- Bell ML, Goldberg R, Hogrefe C, Kinney PL, Knowlton K, Lynn B, Rosenthal J, Rosenzweig C, Patz JA (2007) Climate change, ambient ozone, and health in 50 US cities. Clim Change 82: 61–76
- Brilli F, Barta C, Fortunati A, Lerdau M, Loreto F, Centritto M (2007) Response of isoprene emission and carbon metabolism to drought in white poplar (*Populus alba*) saplings. New Phytol 175: 244–254
- Brilli F, Hörtnagl L, Bamberger I, Schnitzhofer R, Ruuskanen TM, Hansel A, Loreto F, Wohlfahrt G (2012) Qualitative and quantitative characterization of volatile organic compound emissions from cut grass. Environ Sci Technol 46: 3859–3865
- Brilli F, Tsonev T, Mahmood T, Velikova V, Loreto F, Centritto M (2013)
 Ultradian variation of isoprene emission, photosynthesis, mesophyll conductance, and optimum temperature sensitivity for isoprene emission in water-stressed *Eucalyptus citriodora* saplings. J Exp Bot **64:** 519–528
- Brüggemann N, Schnitzler JP (2002) Comparison of isoprene emission, intercellular isoprene concentration and photosynthetic performance in water-limited oak (*Quercus pubescens* Willd. and *Quercus robur* L.) saplings. Plant Biol 4: 456–463
- **Brunner AM, Busov VB, Strauss SH** (2004) Poplar genome sequence: functional genomics in an ecologically dominant plant species. Trends Plant Sci **9**: 49–56
- Ceccato P, Flasse S, Tarantola S, Jacquemoud S, Gregoire JM (2001) Detecting vegetation leaf water content using reflectance in the optical domain. Remote Sens Environ 77: 22–33
- Centritto M, Brilli F, Fodale R, Loreto F (2011) Different sensitivity of isoprene emission, respiration and photosynthesis to high growth temperature coupled with drought stress in black poplar (*Populus nigra*) saplings. Tree Physiol 31: 275–286
- Centritto M, Nascetti P, Petrilli L, Raschi A, Loreto F (2004) Profiles of isoprene emission and photosynthetic parameters in hybrid poplars exposed to free-air CO₂ enrichment. Plant Cell Environ 27: 403–412
- Chaves MM, Maroco JP, Pereira JS (2003) Understanding plant responses to drought: from genes to the whole plant. Funct Plant Biol 30: 239–264
- Cinege G, Louis S, Hänsch R, Schnitzler JP (2009) Regulation of isoprene synthase promoter by environmental and internal factors. Plant Mol Biol 69: 593–604
- Clausen SK, Frenck G, Linden LG, Mikkelsen TN, Lunde C, Jorgensen RB (2011) Effects of single and multifactor treatments with elevated temperature, $\rm CO_2$ and ozone on oilseed rape and barley. J Agron Crop Sci 197: 442–453
- Constable JVH, Guenther AB, Schimel DS, Monson RK (1999) Modelling changes in VOC emission in response to climate change in the continental United States. Glob Change Biol 5: 791–806
- Copolovici L, Niinemets U (2010) Flooding induced emissions of volatile signalling compounds in three tree species with differing waterlogging tolerance. Plant Cell Environ 33: 1582–1594
- Copolovici LO, Filella I, Llusià J, Niinemets U, Peñuelas J (2005) The capacity for thermal protection of photosynthetic electron transport varies for different monoterpenes in *Quercus ilex*. Plant Physiol **139**: 485–496
- Correia B, Pintó-Marijuan M, Neves L, Brossa R, Dias MC, Costa A, Castro BB, Araújo C, Santos C, Chaves MM, et al (2014) Water stress and recovery in the performance of two *Eucalyptus globulus* clones: physiological and biochemical profiles. Physiol Plant 150: 580–592
- Coumou D, Rahmstorf S (2012) A decade of weather extremes. Nat Clim Chang 2: 491–496
- de Gouw JA, Howard CJ, Custer TG, Fall R (1999) Emissions of volatile organic compounds from cut grass and clover are enhanced during the drying process. Geophys Res Lett 26: 811–814

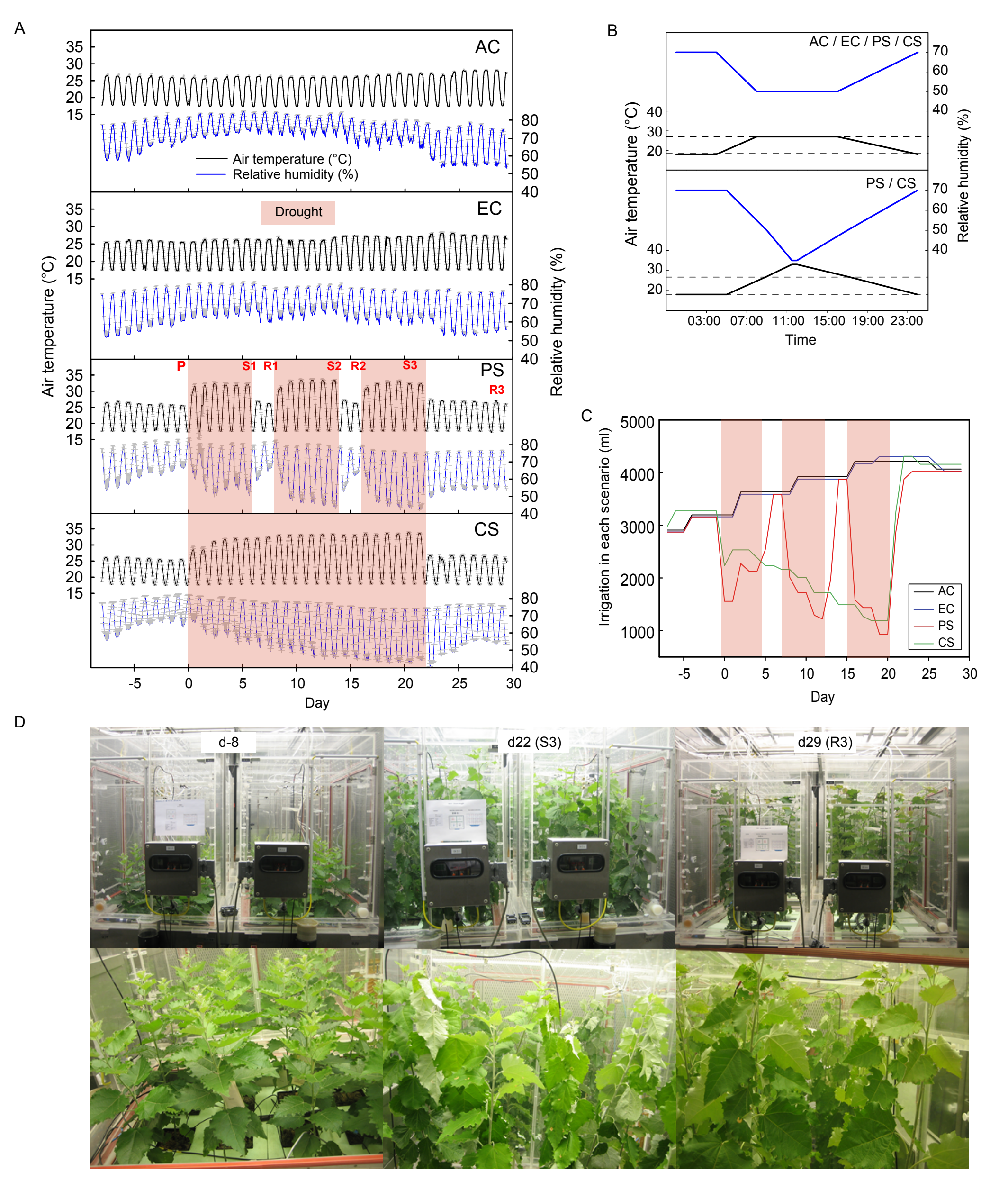
- Eller AS, de Gouw J, Graus M, Monson RK (2012) Variation among different genotypes of hybrid poplar with regard to leaf volatile organic compound emissions. Ecol Appl 22: 1865–1875
- Fall R, Benson AA (1996) Leaf methanol: the simplest natural product from plants. Trends Plant Sci 1: 296–301
- Feussner I, Wasternack C (2002) The lipoxygenase pathway. Annu Rev Plant Biol 53: 275–297
- Feyen L, Dankers R (2009) Impact of global warming on streamflow drought in Europe. J Geophys Res 114: D17116
- Fischer EM, Schär C (2010) Consistent geographical patterns of changes in high-impact European heatwaves. Nat Geosci 3: 398–403
- Fortunati A, Barta C, Brilli F, Centritto M, Zimmer I, Schnitzler JP, Loreto F (2008) Isoprene emission is not temperature-dependent during and after severe drought-stress: a physiological and biochemical analysis. Plant J 55: 687–697
- Gallé A, Feller U (2007) Changes of photosynthetic traits in beech saplings (Fagus sylvatica) under severe drought stress and during recovery. Physiol Plant 131: 412–421
- Genty B, Wonders J, Baker NR (1990) Non-photochemical quenching of Fo in leaves is emission wavelength dependent: consequences for quenching analysis and its interpretation. Photosynth Res 26: 133–139
- Ghirardo A, Gutknecht J, Zimmer I, Brüggemann N, Schnitzler JP (2011)
 Biogenic volatile organic compound and respiratory CO₂ emissions after
 ¹³C-labeling: online tracing of C translocation dynamics in poplar plants.
 PLoS ONE 6: e17393
- Ghirardo A, Heller W, Fladung M, Schnitzler JP, Schroeder H (2012) Function of defensive volatiles in pedunculate oak (*Quercus robur*) is tricked by the moth *Tortrix viridana*. Plant Cell Environ 35: 2192–2207
- Ghirardo A, Koch K, Taipale R, Zimmer I, Schnitzler JP, Rinne J (2010)
 Determination of de novo and pool emissions of terpenes from four common boreal/alpine trees by ¹³CO₂ labelling and PTR-MS analysis.
 Plant Cell Environ 33: 781–792
- Ghirardo A, Wright LP, Bi Z, Rosenkranz M, Pulido P, Rodríguez-Concepción M, Niinemets Ü, Brüggemann N, Gershenzon J, Schnitzler JP (2014) Metabolic flux analysis of plastidic isoprenoid biosynthesis in poplar leaves emitting and nonemitting isoprene. Plant Physiol 165: 37–51
- Graus M, Müller M, Hansel A (2010) High resolution PTR-TOF: quantification and formula confirmation of VOC in real time. J Am Soc Mass Spectrom 21: 1037–1044
- Guenther A, Karl T, Harley P, Wiedinmyer C, Palmer PI, Geron C (2006) Estimates of global terrestrial isoprene emissions using MEGAN (Model of Emissions of Gases and Aerosols from Nature). Atmos Chem Phys 6: 3181–3210
- Hummel I, Pantin F, Sulpice R, Piques M, Rolland G, Dauzat M, Christophe A, Pervent M, Bouteillé M, Stitt M, et al (2010) Arabidopsis plants acclimate to water deficit at low cost through changes of carbon usage: an integrated perspective using growth, metabolite, enzyme, and gene expression analysis. Plant Physiol 154: 357–372
- Hunt ER Jr, Rock BN (1989) Detection of changes in leaf water content using near- and middle-infrared reflectances. Remote Sens Environ 30: 43–54
- Hüve K, Christ MM, Kleist E, Uerlings R, Niinemets U, Walter A, Wildt J (2007) Simultaneous growth and emission measurements demonstrate an interactive control of methanol release by leaf expansion and stomata. J Exp Bot 58: 1783–1793
- IPC (2008) Poplars, willows and people's wellbeing. Report of the 23rd Session of the International Poplar Commission. Beijing, China ftp:// ftp.fao.org/docrep/fao/011/k3380e/k3380e.pdf
- IPCC (2007) Summary for policymakers. In ML Parry, OF Canziani, JP Palutikof, PJ Van der Linden, CE Hanson, eds, Climate Change 2007: Impacts, Adaptation and Vulnerability. Contribution of Working Group II to the Fourth Assessment Report of the Intergovernmental Panel on Climate Change. Cambridge University Press, Cambridge, UK, pp 7–22
- IPCC (2014) Near-term climate change: projections and predictability. In TF Stocker, D Qin, GK Plattner, M Tignor, SK Allen, J Boschung, A Nauels, Y Xia, V Bex, PM Midgley, eds, Climate Change 2013: The Physical Science Basis. Contribution of Working Group I to the Fifth Assessment Report of the Intergovernmental Panel on Climate Change. Cambridge University Press, Cambridge, UK, pp 953–1028
- Jardine KJ, Monson RK, Abrell L, Saleska SR, Arneth A, Jardine A, Ishida FY, Yanez Serrano AM, Artaxo P, Karl T, et al (2012) Withinplant isoprene oxidation confirmed by direct emissions of oxidation

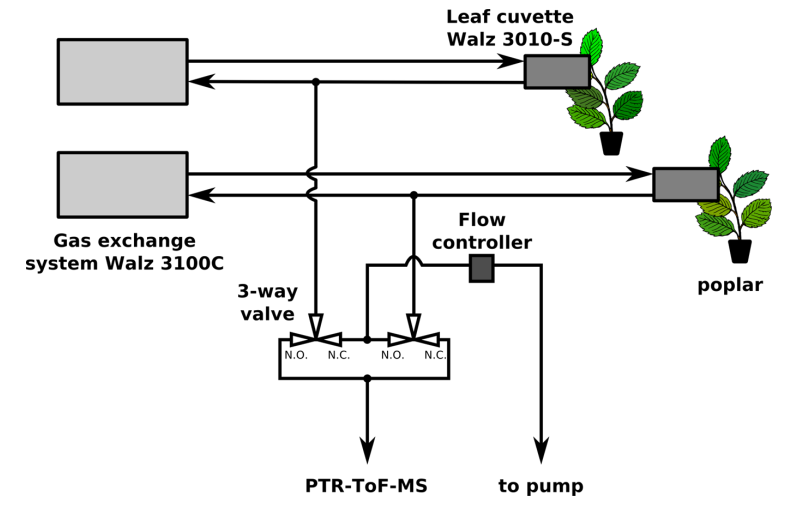
- products methyl vinyl ketone and methacrolein. Glob Change Biol 18: 973–984
- Kirschbaum MUF (1988) Recovery of photosynthesis from water stress in Eucalyptus pauciflora: a process in two stages. Plant Cell Environ 11: 685– 694
- Kreuzwieser J, Scheerer U, Kruse J, Burzlaff T, Honsel A, Alfarraj S, Georgiev P, Schnitzler JP, Ghirardo A, Kreuzer I, et al (2014) The Venus flytrap attracts insects by the release of volatile organic compounds. J Exp Bot 65: 755–766
- Kuokkanen K, Julkunen-Tiitto R, Keinanen M, Niemela P, Tahvanainen J (2001) The effect of elevated ${\rm CO_2}$ and temperature on the secondary chemistry of *Betula pendula* seedlings. Trees **15**: 378–384
- Leplé JC, Brasileiro AC, Michel MF, Delmotte F, Jouanin L (1992) Transgenic poplars: expression of chimeric genes using four different constructs. Plant Cell Rep 11: 137–141
- Levitt J (1980) Stress concepts. *In* TT Kozlowski, ed, Responses of Plants to Environmental Stresses, Ed 2, Vol 2. Academic Press, New York, pp 3–20
- Lichtenthaler HK (1996) Vegetation stress: an introduction to the stress concept in plants. J Plant Physiol 148: 4–14
- Loreto F, Barta C, Brilli F, Nogues I (2006) On the induction of volatile organic compound emissions by plants as consequence of wounding or fluctuations of light and temperature. Plant Cell Environ 29: 1820–1828
- Loreto F, Centritto M, Barta C, Calfapietra C, Fares S, Monson RK (2007)

 The relationship between isoprene emission rate and dark respiration rate in white poplar (*Populus alba* L.) leaves. Plant Cell Environ 30: 662–669
- Loreto F, Schnitzler JP (2010) Abiotic stresses and induced BVOCs. Trends Plant Sci 15: 154–166
- Loreto F, Sharkey TD (1993) Isoprene emission by plants is affected by transmissible wound signals. Plant Cell Environ 16: 563–570
- Loreto F, Velikova V (2001) Isoprene produced by leaves protects the photosynthetic apparatus against ozone damage, quenches ozone products, and reduces lipid peroxidation of cellular membranes. Plant Physiol 127: 1781–1787
- Mahecha MD, Reichstein M, Carvalhais N, Lasslop G, Lange H, Seneviratne SI, Vargas R, Ammann C, Arain MA, Cescatti A, et al (2010) Global convergence in the temperature sensitivity of respiration at ecosystem level. Science 329: 838–840
- Mayrhofer S, Teuber M, Zimmer I, Louis S, Fischbach RJ, Schnitzler JP (2005) Diurnal and seasonal variation of isoprene biosynthesis-related genes in grey poplar leaves. Plant Physiol 139: 474–484
- Mittler R, Zilinskas BA (1994) Regulation of pea cytosolic ascorbate peroxidase and other antioxidant enzymes during the progression of drought stress and following recovery from drought. Plant J 5: 397–405
- Monson RK, Grote R, Niinemets U, Schnitzler JP (2012) Modeling the isoprene emission rate from leaves. New Phytol 195: 541–559
- Monson RK, Jaeger CH, Adams WW, Driggers EM, Silver GM, Fall R (1992) Relationships among isoprene emission rate, photosynthesis, and isoprene synthase activity as influenced by temperature. Plant Physiol 98: 1175–1180
- Monson RK, Trahan N, Rosenstiel TN, Veres P, Moore D, Wilkinson M, Norby RJ, Volder A, Tjoelker MG, Briske DD, et al (2007) Isoprene emission from terrestrial ecosystems in response to global change: minding the gap between models and observations. Philos Trans A Math Phys Eng Sci 365: 1677–1695
- Müller M, Graus M, Ruuskanen TM, Schnitzhofer R, Bamberger I, Kaser L, Titzmann T, Hörtnagl L, Wohlfahrt G, Karl T, et al (2010) First eddy covariance flux measurements by PTR-TOF. Atmos Meas Tech 3: 387– 395
- Murata N, Takahashi S, Nishiyama Y, Allakhverdiev SI (2007) Photoinhibition of photosystem II under environmental stress. Biochim Biophys Acta 1767: 414–421
- Nemecek-Marshall M, MacDonald RC, Franzen JJ, Wojciechowski CL, Fall R (1995) Methanol emission from leaves (enzymatic detection of gas-phase methanol and relation of methanol fluxes to stomatal conductance and leaf development). Plant Physiol 108: 1359–1368
- Niinemets U, Loreto F, Reichstein M (2004) Physiological and physicochemical controls on foliar volatile organic compound emissions. Trends Plant Sci 9: 180–186
- Pegoraro E, Rey A, Bobich EG, Barron-Gafford G, Grieve KA, Malhi Y, Murthy R (2004) Effect of elevated CO₂ concentration and vapour pressure deficit on isoprene emission from leaves of *Populus deltoides* during drought. Funct Plant Biol 31: 1137–1147

- Perkins SE, Alexander LV, Naim JR (2012) Increasing frequency, intensity and duration of observed global heatwaves and warm spells. Geophys Res Lett 39: L20714
- Possell M, Hewitt CN (2011) Isoprene emissions from plants are mediated by atmospheric CO₂ concentrations. Glob Change Biol 17: 1595–1610
- Potosnak MJ, Lestourgeon L, Nunez O (2014) Increasing leaf temperature reduces the suppression of isoprene emission by elevated CO₂ concentration. Sci Total Environ 481: 352–359
- Rasulov B, Hüve K, Bichele I, Laisk A, Niinemets U (2010) Temperature response of isoprene emission in vivo reflects a combined effect of substrate limitations and isoprene synthase activity: a kinetic analysis. Plant Physiol 154: 1558–1570
- Rennenberg H, Loreto F, Polle A, Brilli F, Fares S, Beniwal RS, Gessler A (2006) Physiological responses of forest trees to heat and drought. Plant Biol (Stuttg) 8: 556–571
- Rosenkranz M, Pugh TAM, Schnitzler JP, Arneth A (November 15, 2014) Effect of land-use change and management on BVOC emissions: selecting climate-smart cultivars. Plant Cell Environ 38: 1896–1912
- Rosenstiel TN, Potosnak MJ, Griffin KL, Fall R, Monson RK (2003) Increased CO_2 uncouples growth from isoprene emission in an agriforest ecosystem. Nature 421: 256–259
- Ryan AC, Hewitt CN, Possell M, Vickers CE, Purnell A, Mullineaux PM, Davies WJ, Dodd IC (2014) Isoprene emission protects photosynthesis but reduces plant productivity during drought in transgenic tobacco (*Nicotiana tabacum*) plants. New Phytol **201**: 205–216
- Sales CR, Ribeiro RV, Silveira JA, Machado EC, Martins MO, Lagôa AM (2013) Superoxide dismutase and ascorbate peroxidase improve the recovery of photosynthesis in sugarcane plants subjected to water deficit and low substrate temperature. Plant Physiol Biochem 73: 326–336
- Schnitzler JP, Zimmer I, Bachl A, Arend M, Fromm J, Fischbach RJ (2005)
 Biochemical properties of isoprene synthase in poplar (*Populus* × *canescens*).
 Planta 222: 777–786
- Scholander PF, Bradstreet ED, Hemmingsen EA, Hammel HT (1965) Sap pressure in vascular plants: negative hydrostatic pressure can be measured in plants. Science 148: 339–346
- Seckmeyer GP, Payer HD (1993) A new sunlight simulator for ecological research on plants. J Photochem Photobiol B 21: 175–181
- Sharkey TD, Chen X, Yeh S (2001) Isoprene increases thermotolerance of fosmidomycin-fed leaves. Plant Physiol 125: 2001–2006
- Sharkey TD, Yeh S (2001) Isoprene emission from plants. Annu Rev Plant Physiol Plant Mol Biol 52: 407–436
- Singsaas EL, Lerdau M, Winter K, Sharkey TD (1997) Isoprene increases thermotolerance of isoprene-emitting species. Plant Physiol 115: 1413–1420
- Singsaas EL, Sharkey TD (1998) The regulation of isoprene emission responses to rapid leaf temperature fluctuations. Plant Cell Environ 21: 1181–1188
- Sofo A, Dichio B, Xiloyannis C, Masia A (2004) Effects of different irradiance levels on some antioxidant enzymes and on malondialdehyde content during rewatering in olive tree. Plant Sci 166: 293–302
- Sun Z, Niinemets Ü, Hüve K, Rasulov B, Noe SM (2013) Elevated atmospheric CO₂ concentration leads to increased whole-plant isoprene emission in hybrid aspen (*Populus tremula* × *Populus tremuloides*). New Phytol **198**: 788–800
- Takahashi S, Murata N (2008) How do environmental stresses accelerate photoinhibition? Trends Plant Sci 13: 178–182
- Tattini M, Velikova V, Vickers C, Brunetti C, Di Ferdinando M, Trivellini A, Fineschi S, Agati G, Ferrini F, Loreto F (2014) Isoprene production in transgenic tobacco alters isoprenoid, non-structural carbohydrate and phenylpropanoid metabolism, and protects photosynthesis from drought stress. Plant Cell Environ 37: 1950–1964
- Thiel S, Döhring T, Köfferlein M, Kosak A, Martin P, Seidlitz HK (1996)
 A phytotron for plant stress research: how far can artificial lighting compare to natural sunlight? J Plant Physiol 148: 456–463

- Thornton PK, Ericksen PJ, Herrero M, Challinor AJ (2014) Climate variability and vulnerability to climate change: a review. Glob Change Biol 20: 3313–3328
- Trowbridge AM, Asensio D, Eller ASD, Way DA, Wilkinson MJ, Schnitzler JP, Jackson RB, Monson RK (2012) Contribution of various carbon sources toward isoprene biosynthesis in poplar leaves mediated by altered atmospheric CO₂ concentrations. PLoS ONE 7: e32387
- Tschaplinski TJ, Tuskan GA, Gebre GM, Todd DE (1998) Drought resistance of two hybrid *Populus* clones grown in a large-scale plantation. Tree Physiol 18: 653–658
- Tuskan GA, Difazio S, Jansson S, Bohlmann J, Grigoriev I, Hellsten U, Putnam N, Ralph S, Rombauts S, Salamov A, et al (2006) The genome of black cottonwood, *Populus trichocarpa* (Torr. & Gray). Science 313: 1506–1604
- Velikova V, Ghirardo A, Vanzo E, Merl J, Hauck SM, Schnitzler JP (2014)
 Genetic manipulation of isoprene emissions in poplar plants remodels the chloroplast proteome. J Proteome Res 13: 2005–2018
- Velikova V, Müller C, Ghirardo A, Rock TM, Aichler M, Walch A, Schmitt-Kopplin P, Schnitzler JP (2015) Knocking down of isoprene emission modifies the lipid matrix of thylakoid membranes and influences the chloroplast ultrastructure in poplar. Plant Physiol 168: 859–870
- Velikova V, Pinelli P, Loreto F (2005) Consequences of inhibition of isoprene synthesis in *Phragmites australis* leaves exposed to elevated temperatures. Agric Ecosyst Environ 106: 209–217
- Velikova V, Várkonyi Z, Szabó M, Maslenkova L, Nogues I, Kovács L, Peeva V, Busheva M, Garab G, Sharkey TD, et al (2011) Increased thermostability of thylakoid membranes in isoprene-emitting leaves probed with three biophysical techniques. Plant Physiol 157: 905–916
- Vickers CE, Possell M, Cojocariu CI, Velikova VB, Laothawornkitkul J, Ryan A, Mullineaux PM, Hewitt CN (2009) Isoprene synthesis protects transgenic tobacco plants from oxidative stress. Plant Cell Environ 32: 520–531
- von Caemmerer S, Farquhar GD (1981) Some relationships between the biochemistry of photosynthesis and the gas exchange of leaves. Planta 153: 376–387
- Way DA, Ghirardo A, Kanawati B, Esperschütz J, Monson RK, Jackson RB, Schmitt-Kopplin P, Schnitzler JP (2013) Increasing atmospheric CO₂ reduces metabolic and physiological differences between isopreneand non-isoprene-emitting poplars. New Phytol **200**: 534–546
- Way DA, Schnitzler JP, Monson RK, Jackson RB (2011) Enhanced isoprene-related tolerance of heat- and light-stressed photosynthesis at low, but not high, CO₂ concentrations. Oecologia **166**: 273–282
- **Way DA, Yamori W** (2014) Thermal acclimation of photosynthesis: on the importance of adjusting our definitions and accounting for thermal acclimation of respiration. Photosynth Res **119**: 89–100
- Wiberley AE, Donohue AR, Westphal MM, Sharkey TD (2009) Regulation of isoprene emission from poplar leaves throughout a day. Plant Cell Environ 32: 939–947
- Wiberley AE, Linskey AR, Falbel TG, Sharkey TD (2005) Development of the capacity for isoprene emission in kudzu. Plant Cell Environ 28: 898– 905
- Wilkinson MJ, Monson RK, Trahan N, Lee S, Brown E, Jackson RB, Polley HW, Fay PA, Fall R (2009) Leaf isoprene emission rate as a function of atmospheric CO₂ concentration. Glob Change Biol 15: 1189– 1200
- Wullschleger SD, Jansson S, Taylor G (2002) Genomics and forest biology: *Populus* emerges as the perennial favorite. Plant Cell **14**: 2651–2655
- Wuyts N, Palauqui JC, Conejero G, Verdeil JL, Granier C, Massonnet C (2010) High-contrast three-dimensional imaging of the Arabidopsis leaf enables the analysis of cell dimensions in the epidermis and mesophyll. Plant Methods 6: 17
- Zhu XG, Song Q, Ort DR (2012) Elements of a dynamic systems model of canopy photosynthesis. Curr Opin Plant Biol 15: 237–244





Ε

Figure S1. Time courses of air temperature, relative humidity, irrigation and plant appearance in the four scenarios. A, Diurnal course of air temperature and relative humidity during the experiment. The given values are the means of 4 sub-chambers (± SE). B, Theoretical values of daily air temperature and relative humidity when maximum air temperature was set to 27 °C (pre-stress and recovery, above) and to 33 °C during stress in PS and CS (below). Dashed lines indicate mean night temperature (18 °C) and light hour air temperature under unstressed conditions (27 °C). C. Irrigation profile of the experiment. Water amount (in ml) is given to the pots by automated drip irrigation systems. Values represent means of the 4 sub-chambers (representing each genotype) within each scenario (AC, EC, PS, CS). D, Front view of 2 sub-chambers (scenario PS) with12 Grey poplar plants arranged within 1 subchamber. E, Schematic of the setup used for the leaf-level gas exchange and VOC emission measurements. The PTR-ToF-MS was sampling from the leaf cuvette backstream line and could be switched to sample from either gas exchange system. AC = control ambient [CO₂], EC = control elevated [CO₂], PS = periodic stress, CS = chronic stress.

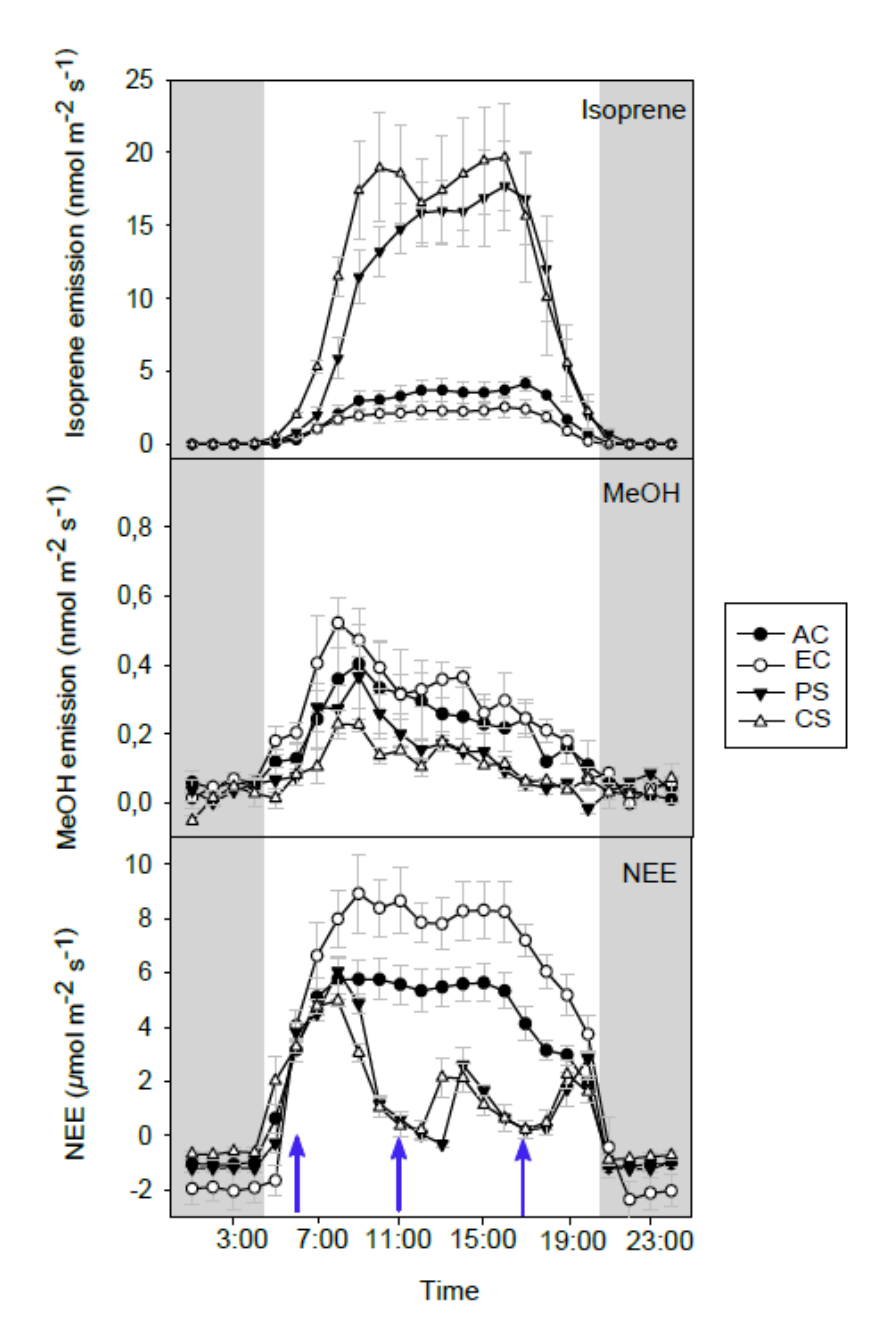


Figure S2. Representative day (d20) showing the CL isoprene emission (NIE), MeOH emission and net ecosystem exchange (NEE). Blue arrows indicate time points of irrigation in the 4 scenarios (6:00; 12:00; 18:00, MEZ). Amount of water in AC and EC was higher than in PS and CS. Values for each scenario and treatments are given as mean of 4 sub-chambers (\pm SE). Dark hours are highlighted in grey. AC = control ambient [CO₂], EC = control elevated [CO₂], PS = periodic stress, CS = chronic stress.

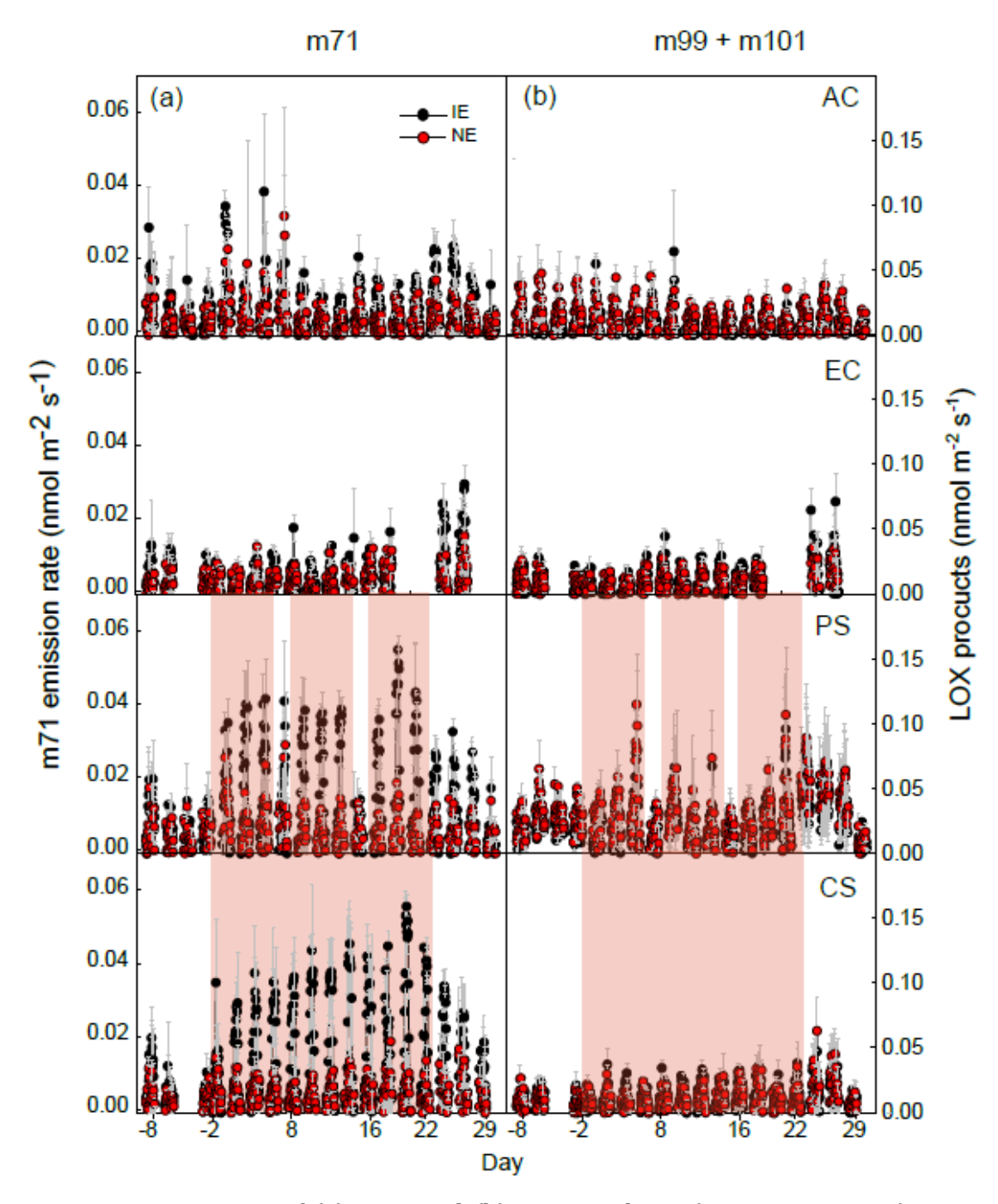


Figure S3. Time course of (a) m71 and (b) LOX products (i.e. m99 + m101) emission rates of IE (black circles) and NE (red circles) poplar genotypes in the four scenarios (AC, EC, PS, CS). Measurements were performed on the CL. Periods of HDS are highlighted in red. Values represent means of $n = 4 \pm SE$.

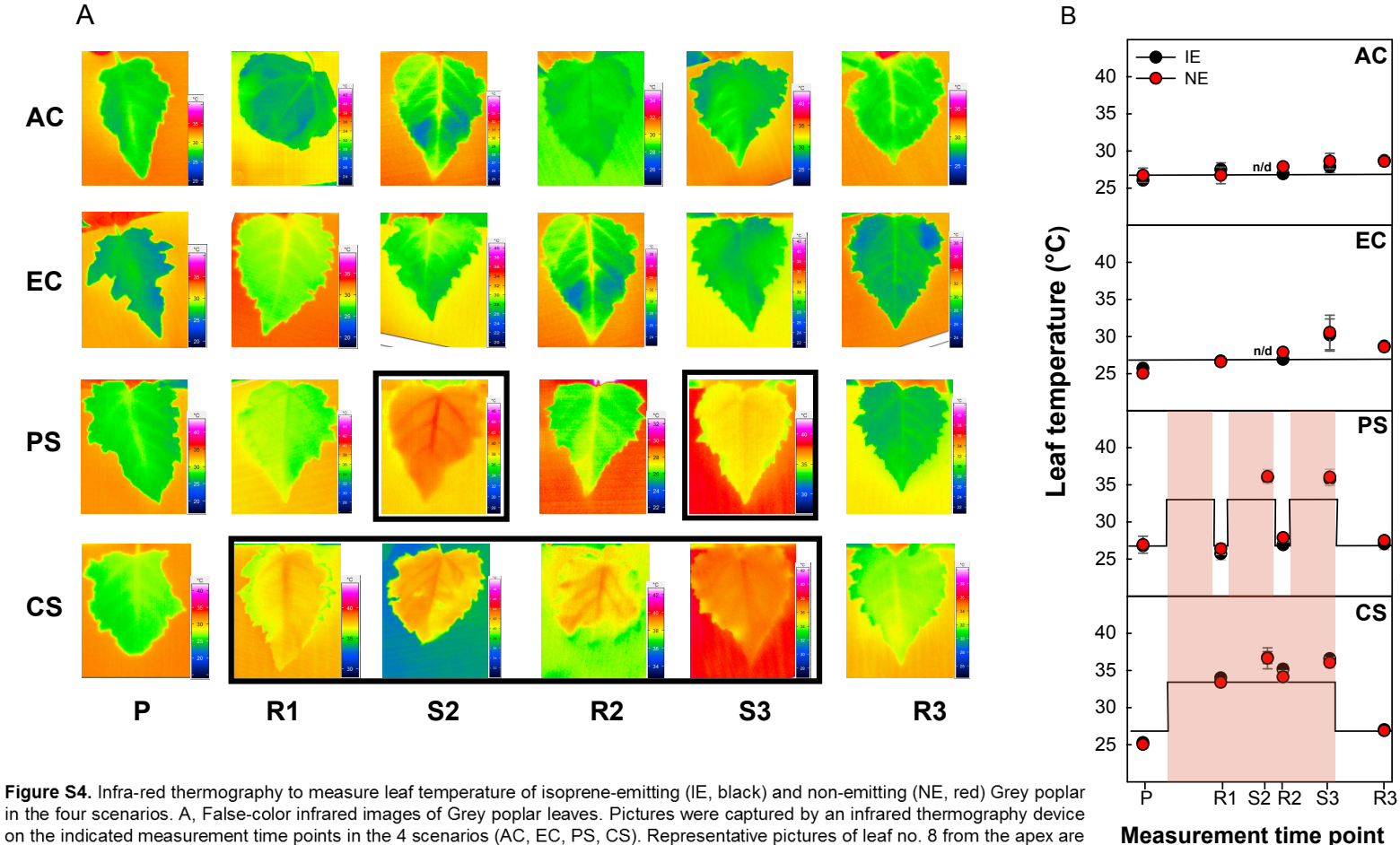


Figure S4. Infra-red thermography to measure leaf temperature of isoprene-emitting (IE, black) and non-emitting (NE, red) Grey poplar in the four scenarios. A, False-color infrared images of Grey poplar leaves. Pictures were captured by an infrared thermography device on the indicated measurement time points in the 4 scenarios (AC, EC, PS, CS). Representative pictures of leaf no. 8 from the apex are given. Black frames indicate heat and drought spells in the PS and CS scenario. B, Effect of 4 scenarios on the leaf temperature of isoprene-emitting (IE, black circles) and non-emitting (NE, red circles) poplar genotypes. Values represent means (± SE) of measurements performed in four sub-chambers; dashed lines denote the maximum air temperature during the light hours in the different scenarios. Thermal images were obtained using a thermographic digital camera (VarioCAM basic, Jenoptic Laser, Jena, Germany); pictures were taken from the adaxial side on the 8th leaf from the top at the time points P, R1, S2, R2, S3 and R3. Digital thermograms were analyzed with the IRBIS Plus software package (v. 2.2 Infratec, Dresden, Germany).

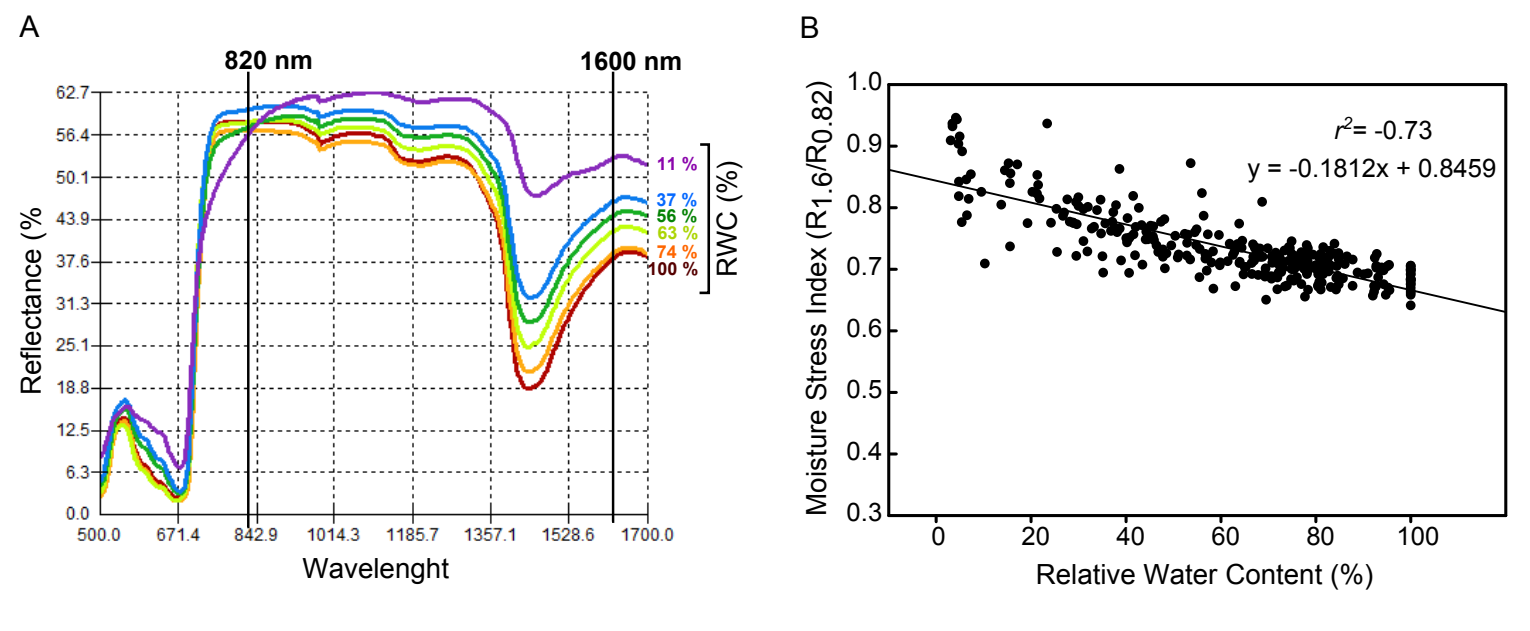
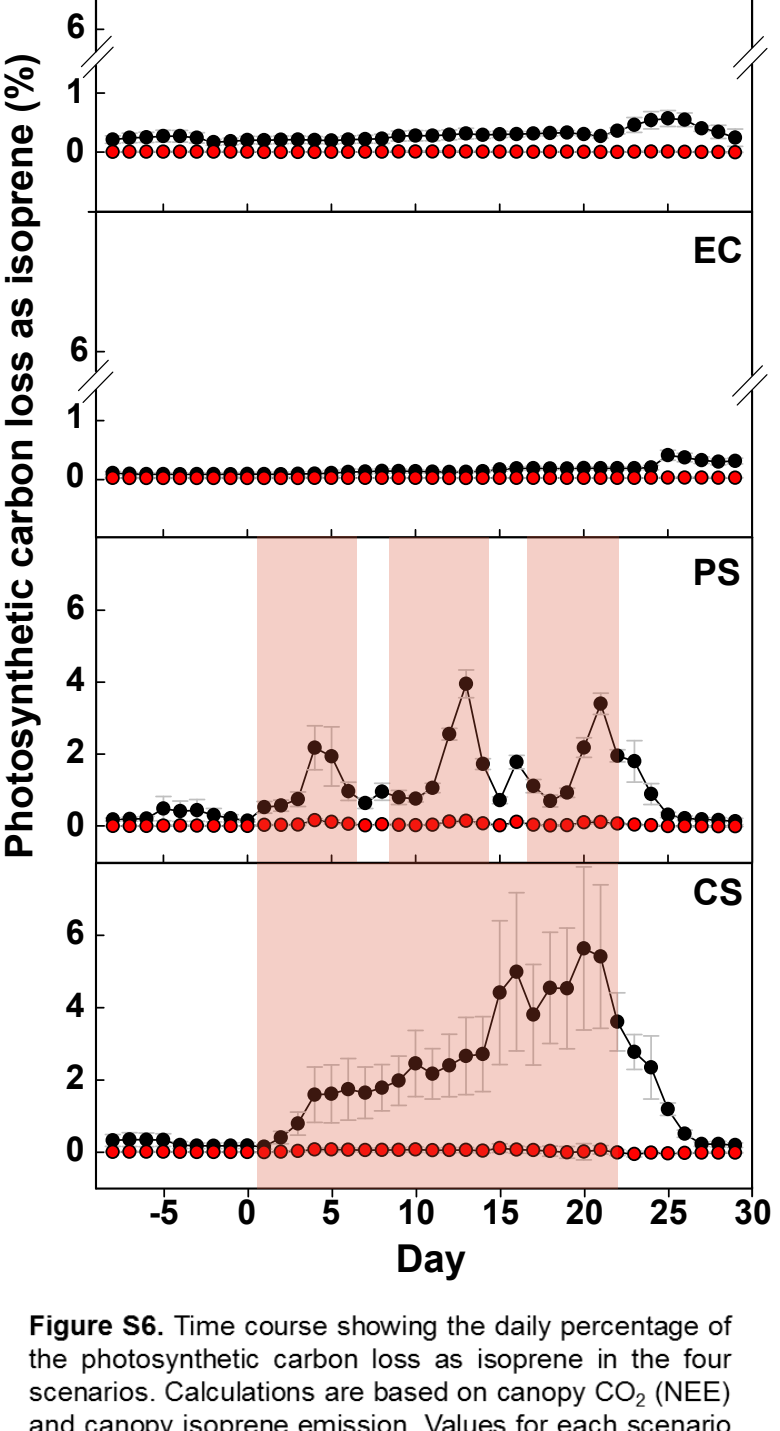


Figure S5. Drying experiment to assess the Moisture Stress Index and the Relative Water Context of Grey poplar leaves. A, Representative spectra of a leaf of Grey poplar during drying. Corresponding relative water contents (RWC) are given. Leaf reflectance was measured by near infrared spectrometry device, RWC was calculated based on the hourly leaf weight according the following equation: (FreshWeight-DryWeight)/(FreshWeight₀-DryWeight). Wavelengths of 820 nm and 1600 nm (vertical lines) were used for calculation of the Moisture Stress Index (MSI = Reflectance₁₆₀₀/Reflectance₈₂₀). B, Relationship of the MSI to the RWC of drying leaves of Grey poplar. Five plants of each isoprene-emitting and non-emitting poplar genotype were examined hourly by NIR reflectance. Regression equation and coefficient of correlation are given.



IE NE AC

the photosynthetic carbon loss as isoprene in the four scenarios. Calculations are based on canopy CO_2 (NEE) and canopy isoprene emission. Values for each scenario are given as mean of n = 4 (\pm SE). The scenarios are: AC = control with ambient [CO_2], EC = control with elevated [CO_2], PS = periodic stress, CS = chronic stress. Periods of heat and drought are indicated in red.

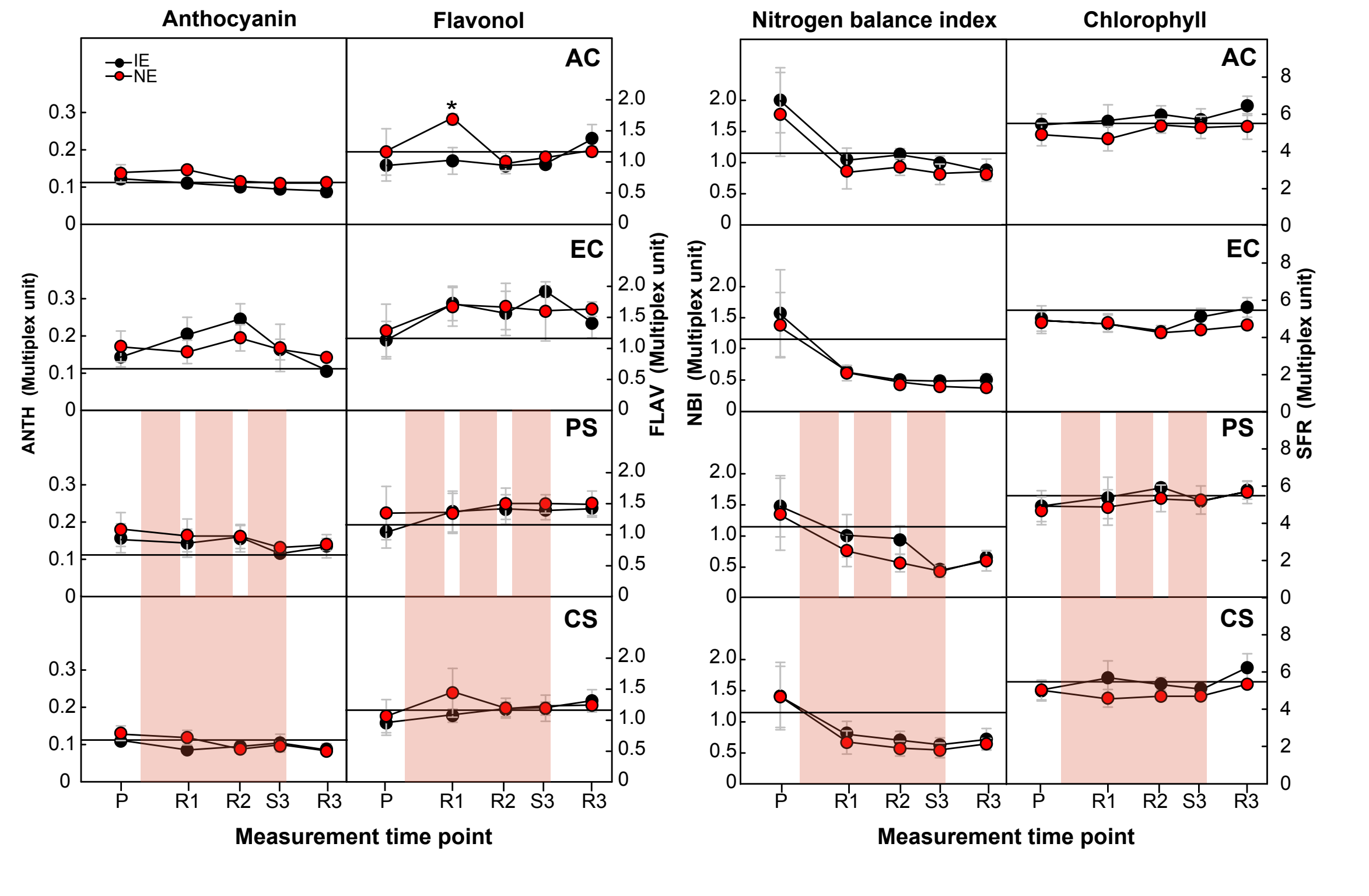


Figure S7. Effect of four scenarios on the anthocyanin index, flavonol index, nitrogen balance index (NBI®) and chlorophyll index of isoprene-emitting (IE, black circles) and non-emitting (NE, red circles) poplar genotypes. Measurement of the pigments was performed weekly by Multiplex® optical sensor (Force-A, Orsay, France). Values represent means (± SE) of measurements performed in 4 sub-chambers; dashed lines indicate an arbitrary reference value. Asterisks indicate significant genotype differences within each scenario and time point (*P* < 0.05). Multiplex® optical sensor: The fluorescence signals are measured in the red (RF) and far-red (FRF) spectral regions excited under ultraviolet (UV), green (G) or red (R) radiation (in the following equations the subscripted characters indicate the excitation radiation). The simple chlorophyll fluorescence ratio (SFR) of far-red emission (735 nm) divided by red emission (685 nm) is linked to the chlorophyll content of the sample (Lichtenthaler et al., 1986; Buschmann, 2007). The flavonol index (FLAV), calculated according to equation FLAV = log(FRF_R/FRF_{UV}), is proportional to the flavonol content of the leaf (Cerovic et al., 2002). Other fluorescence-based indices like the anthocyanin index ANTH = log(FRF_R/FRF_G) and the nitrogen balance index NBI = FRF_{UV}/RF_G are also described in literature (Meyer et al., 2006; Agati et al., 2007). Multiplex® measurements were performed in situ under ambient light conditions on the time points pre-stress (P), recovery phase 1 (R1), recovery phase 2 (R2), stress cycle 3 (S3), and recovery phase 3 (R3) on 6 plants per genotype and scenario. A constant distance between sensor and leaves was kept at all measurements using a grid in front of the sensor.

1 Supplemental Tables

- Table S1. Results of two-way ANOVAs and Bonferroni post-hoc tests for all measured parameters. Significant differences are marked in red when
- 3 P < 0.05.

												Scer	nario (effect									
			n effe otypes			Maiı	ı scen	ario e	effect	(IE +	NE)	IE						NE					
	Time points	AC	EC	PS	CS	AC vs EC	AC vs PS	AC vs CS	EC vs PS	EC vs CS	PS vs CS	AC vs EC	AC vs PS	AC vs CS	EC vs PS	EC vs CS	PS vs CS	AC vs EC	AC vs PS	AC vs CS	EC vs PS	EC vs CS	PS vs CS
											\mathbf{C}	anop	y-lev	/el									
Net ecosystem exchange (NEE)	all time points	0.191	0.320	0.089	0.009	0.001	0.412	0.001	0.010	< 0.001	< 0.001						-	-					-
	P	0.348	0.961	0.205	0.372	1.000	0.172	1.000	0.532	1.000	0.164	1.000	0.988	1.000	1.000	1.000	1.000	1.000	0.517	1.000	0.544	1.000	0.052
	S1	0.338	0.566	0.700	0.542	1.000	< 0.001	< 0.001	< 0.001	< 0.001	1.000	1.000	0.045	0.051	0.004	0.005	1.000	1.000	0.008	< 0.001	0.088	0.009	1.000
	R1	0.531	0.499 0.899	0.967 0.425	0.605 0.789	0.768 1.000	0.018 < 0.001	< 0.001 < 0.001	1.000	< 0.001 < 0.001	< 0.001	0.515 1.000	0.088	0.019 0.014	1.000	< 0.001 0.002	< 0.001	1.000	0.441 < 0.001	< 0.001	1.000	0.001	< 0.001
	S2 R2	0.846	0.899	0.423	0.789	0.278	< 0.001	< 0.001	0.001	0.001	1.000	0.376	< 0.001	< 0.014	0.001	0.002	1.000	1.000	0.001	0.001	0.408	0.705	1.000
	S3	0.985	0.793	0.643	0.511	1.000	< 0.001	< 0.001	< 0.004	< 0.001	1.000	1.000	0.001	0.001	0.013	0.002	1.000	1.000	< 0.001	< 0.001	< 0.001	< 0.001	1.000
	R3	0.846	0.516	0.016	0.042	0.278	< 0.001	< 0.001	0.004	0.028	1.000	0.376	< 0.001	< 0.001	0.015	0.082	1.000	1.000	0.005	0.014	0.408	0.705	1.000
Evapotranspiration	all time	0.001	0.023	< 0.001	< 0.001	< 0.001	0.466	< 0.001	< 0.001	< 0.001	< 0.001												
	P	0.710	< 0.001	0.523	0.011	< 0.001	0.001	0.573	< 0.001	< 0.001	0.186	< 0.001	0.167	0.142	< 0.001	< 0.001	1.000	1.000	0.009	1.000	1.000	1.000	0.012
	S1	< 0.001	< 0.001	< 0.001	0.021	< 0.001	< 0.001	< 0.001	< 0.001	< 0.001	0.240	< 0.001	0.005	< 0.001	< 0.001	< 0.001	< 0.001	1.000	< 0.001	0.092	< 0.001	0.023	0.157
	R1	0.001	< 0.001	< 0.001	0.118	0.002	0.594	< 0.001	0.139	< 0.001	< 0.001	< 0.001	0.528	< 0.001	0.007	< 0.001	< 0.001	1.000	1.000	0.222	1.000	0.187	0.042
	S2	0.012	< 0.001	< 0.001	0.736	0.006	< 0.001	< 0.001	< 0.001	< 0.001	1.000	0.004	0.001	< 0.001	< 0.001	< 0.001	0.726	1.000	< 0.001	0.059	< 0.001	0.005	0.021
	R2	0.525	0.007	0.031	0.836	1.000	1.000	< 0.001	1.000	< 0.001	< 0.001	0.034	0.180	< 0.001	1.000	< 0.001	< 0.001	1.000	1.000	< 0.001	1.000	< 0.001	< 0.001
	S3	0.979	0.012	0.020	0.857	0.267	< 0.001	< 0.001	< 0.001	< 0.001	1.000	0.025	0.013	< 0.001	< 0.001	< 0.001	0.706	1.000	< 0.001	< 0.001	< 0.001	0.002	1.000
	R3	0.901	0.077	0.550	0.138	0.295	< 0.001	< 0.001	0.001	0.900	0.017	0.112	< 0.001	0.002	0.288	1.000	0.544	1.000	< 0.001	0.141	0.003	0.908	0.063
Water use efficiency (WUE), canopy	all time points	< 0.001	0.003	< 0.001	< 0.001	0.099	1.000	1.000	0.007	0.001	1.000	-			-		-	-				-	-
	P	0.133	0.112	0.360	0.465	1.000	1.000	1.000	1.000	1.000	1.000	1.000	1.000	1.000	1.000	1.000	1.000	1.000	1.000	1.000	1.000	1.000	1.000
	S1	0.010	0.059	< 0.001	< 0.001	1.000	0.131	< 0.001	0.004	< 0.001	0.041	1.000	1.000	< 0.001	1.000	< 0.001	< 0.001	1.000	0.003	1.000	< 0.001	1.000	< 0.001
	R1	0.016	0.080	0.405	0.014	1.000	1.000	1.000	1.000	0.423	0.500	1.000	1.000	0.016	1.000	0.005	0.026	1.000	0.924	0.390	1.000	1.000	1.000
	S2	0.041	0.210	< 0.001	0.258	1.000	< 0.001	1.000	< 0.001	1.000	< 0.001	1.000	1.000	0.377	1.000	0.216	0.237	1.000	< 0.001	1.000	< 0.001	1.000	< 0.001
	R2 S3	0.062	0.608 0.612	0.970 0.904	0.546 0.556	1.000	0.863	1.000	1.000	1.000 1.000	1.000	1.000	1.000	1.000 1.000	1.000 1.000	1.000	1.000	0.801 1.000	0.312 1.000	0.368	1.000 1.000	1.000	1.000 1.000
	R3	0.248	0.612	0.843	0.895	1.000	1.000	1.000	1.000 1.000	1.000	1.000	1.000	1.000	1.000	1.000	1.000	1.000	1.000	1.000	0.652 1.000	1.000	1.000 1.000	1.000
Electron transport rate (ETR) leaf4	all time	0.677	0.729	0.017	0.344	1.000	0.793	1.000	0.177	1.000	0.063												
	P	0.967	0.496	0.984	0.735	1.000	1.000	1.000	1.000	1.000	1.000	1.000	1.000	1.000	1.000	1.000	1.000	1.000	1.000	1.000	1.000	1.000	1.000
	S1	n/d	n/d	0.686	0.755	n/d	n/d	n/d	n/d	n/d	0.496		1.000				0.902						0.402
	R1	0.927	0.967	0.955	0.842	1.000	0.554	1.000	0.149	1.000	0.380	1.000	1.000	1.000	1.000	0.677	1.000	1.000	1.000	1.000	0.656	1.000	0.892

1	S2	n/d	n/d	0.019	0.399	n/d	n/d	n/d	n/d	n/d	0.001	ı					0.122	i					0.003
	R2	0.739	0.422	0.202	0.160	1.000	1.000	1.000	1.000	1.000	1.000	0.779	1.000	0.580	1.000	1.000	1.000	1.000	1.000	1.000	1.000	1.000	1.000
	S3	0.770	0.951	0.051	0.126	1.000	1.000	1.000	1.000	1.000	1.000	1.000	1.000	1.000	1.000	1.000	1.000	1.000	0.936	1.000	1.000	1.000	1.000
	R3	0.307	0.898	0.759	0.667	1.000	1.000	1.000	1.000	1.000	1.000	1.000	1.000	1.000	1.000	1.000	1.000	1.000	1.000	1.000	1.000	1.000	1.000
	all time			0.757		1.000	1.000					1.000	1.000	1.000	1.000	1.000	1.000	1.000	1.000	1.000	1.000	1.000	1.000
ETR leaf8	points	0.231	0.451	< 0.001	0.001	0.164	< 0.001	0.647	0.044	1.000	0.001												
	points	0.735	0.894	0.742	0.629	1.000	1.000	0.374	1.000	1.000	0.850	1.000	1.000	1.000	1.000	1.000	1.000	1.000	1.000	0.504	1.000	1.000	0.893
	S1	0.733	0.074	0.024	0.758	n/d	n/d	n/d	n/d	n/d	0.566	1.000	1.000	1.000	1.000	1.000	0.565	1.000	1.000	0.504	1.000	1.000	0.167
	R1	0.984	0.742	0.735	0.622	1.000	1.000	1.000	1.000	1.000	0.334	1.000	1.000	1.000	1.000	1.000	0.462	1.000	1.000	1.000	1.000	1.000	1.000
	S2	0.704	0.742	< 0.001	0.003	n/d	n/d	n/d	n/d	n/d	< 0.001	1.000	1.000	1.000	1.000	1.000	0.074	1.000	1.000	1.000	1.000	1.000	< 0.001
	R2	0.593	0.926	0.291	0.007	1.000	0.536	0.265	1.000	0.815	1.000	1.000	1.000	1.000	1.000	1.000	1.000	1.000	0.024	0.072	1.000	0.109	1.000
	S3	0.255	0.412	0.014	0.005	0.004	< 0.001	0.001	0.016	1.000	0.048	0.054	0.001	0.353	1.000	1.000	0.242	0.128	< 0.001	0.003	0.020	0.023	0.515
	R3	0.518	0.758	0.681	0.934	0.256	1.000	1.000	0.227	0.544	1.000	0.649	1.000	1.000	0.763	1.000	1.000	1.000	1.000	1.000	0.982	0.982	1.000
	all time	0.510	0.750	0.001	0.754	0.230	1.000	1.000	0.227	0.544	1.000	0.042	1.000	1.000	0.703	1.000	1.000	1.000	1.000	1.000	0.702	0.702	1.000
ETR leaf12	points	0.453	0.746	< 0.001	0.010	1.000	< 0.001	0.113	< 0.001	0.234	0.014	-	-	-		-	-	-		•		-	-
	P	0.969	0.938	0.897	0.796	0.439	1.000	0.743	0.995	1.000	1.000	1.000	1.000	1.000	1.000	1.000	1.000	1.000	1.000	1.000	1.000	1.000	1.000
	S1	n/d	n/d	0.387	0.959	n/d	n/d	n/d	n/d	n/d	0.482	n/d	n/d	n/d	n/d	n/d	0.969	n/d	n/d	n/d	n/d	n/d	0.339
	R1	0.928	0.990	0.642	0.938	1.000	1.000	1.000	0.374	1.000	1.000	1.000	1.000	1.000	0.715	1.000	1.000	1.000	1.000	1.000	1.000	1.000	1.000
	S2	n/d	n/d	< 0.001	0.038	n/d	n/d	n/d	n/d	n/d	< 0.001	n/d	n/d	n/d	n/d	n/d	0.006	n/d	n/d	n/d	n/d	n/d	< 0.001
	R2	0.866	0.948	0.333	0.023	1.000	0.252	0.122	0.338	0.169	1.000	1.000	1.000	1.000	1.000	1.000	1.000	1.000	0.396	0.044	0.374	0.041	1.000
	S3	0.623	0.806	0.001	0.020	0.119	< 0.001	< 0.001	< 0.001	0.009	1.000	0.263	0.004	0.018	0.872	1.000	1.000	1.000	< 0.001	< 0.001	< 0.001	0.003	1.000
	R3	0.251	0.727	0.172	0.679	1.000	1.000	1.000	1.000	1.000	1.000	0.894	1.000	1.000	0.831	1.000	1.000	1.000	1.000	1.000	1.000	1.000	1.000
Isoprene emission, canopy	all time	< 0.001	0.033	< 0.001	0.000	0.057	< 0.001	< 0.001	< 0.001	< 0.001	0.002							-				-	-
	P	0.112	0.703	0.155	0.159	0.853	1.000	1.000	1.000	1.000	1.000	1.000	1.000	1.000	1.000	1.000	1.000	1.000	1.000	1.000	1.000	1.000	1.000
	S1	0.126	0.577	< 0.001	< 0.001	1.000	0.084	0.100	0.073	0.078	1.000	1.000	0.008	0.004	0.007	0.003	1.000	1.000	1.000	1.000	1.000	1.000	1.000
	R1	0.117	0.473	0.051	< 0.001	1.000	1.000	< 0.001	1.000	0.001	0.001	1.000	1.000	< 0.001	1.000	< 0.001	< 0.001	1.000	1.000	1.000	1.000	1.000	1.000
	S2	0.063	0.503	< 0.001	< 0.001	1.000	< 0.001	< 0.001	< 0.001	< 0.001	1.000	1.000	< 0.001	< 0.001	< 0.001	< 0.001	1.000	1.000	1.000	1.000	1.000	1.000	1.000
	R2	0.065	0.394	0.001	< 0.001	1.000	1.000	< 0.001	1.000	< 0.001	0.002	1.000	0.782	< 0.001	0.419	< 0.001	< 0.001	1.000	1.000	1.000	1.000	1.000	1.000
	S3	0.058	0.412	< 0.001	< 0.001	1.000	0.002	< 0.001	0.004	< 0.001	1.000	1.000	< 0.001	< 0.001	< 0.001	< 0.001	0.366	1.000	1.000	1.000	1.000	1.000	1.000
	R3	0.009	0.094	0.006	0.003	1.000	1.000	1.000	1.000	1.000	1.000	1.000	1.000	1.000	1.000	1.000	1.000	1.000	1.000	1.000	1.000	1.000	1.000
	all time																						
Methanol emission, canopy	points	0.048	0.037	0.284	0.466	0.077	< 0.001	< 0.001	< 0.001	< 0.001	1.000			•			-	-		•			-
	P	0.040	0.898	0.135	0.885	1.000	1.000	1.000	1.000	0.241	0.351	0.591	1.000	1.000	1.000	1.000	1.000	1.000	1.000	0.437	1.000	0.674	0.188
	S1	0.420	0.789	0.624	0.684	1.000	0.096	0.204	1.000	1.000	1.000	1.000	0.719	1.000	1.000	1.000	1.000	1.000	0.372	0.214	1.000	1.000	1.000
	R1	0.351	0.355	0.595	0.873	1.000	0.798	0.038	0.247	0.014	1.000	0.810	1.000	0.961	0.172	0.053	1.000	1.000	1.000	0.080	1.000	0.532	1.000
	S2	0.493	0.396	0.798	0.515	0.414	0.022	0.067	< 0.001	0.001	1.000	0.243	0.378	1.000	0.003	0.019	1.000	1.000	0.135	0.084	0.105	0.070	1.000
	R2	0.809	0.305	0.876	0.697	1.000	0.140	0.014	0.022	0.002	1.000	0.871	0.701	0.372	0.040	0.019	1.000	1.000	0.591	0.079	0.919	0.210	1.000
	S3	0.957	0.167	0.789	0.920	0.127	0.143	0.286	< 0.001	0.001	1.000	0.088	0.523	1.000	0.001	0.003	1.000	1.000	0.802	0.831	0.250	0.259	1.000
	R3	0.624	0.077	0.715	0.939	0.010	1.000	1.000	0.009	0.011	1.000	0.004	1.000	1.000	0.011	0.009	1.000	1.000	1.000	1.000	0.960	1.000	1.000
Relative water content (RWC) leaf4	all time points	0.406	0.445	0.972	0.888	0.030	0.123	1.000	1.000	0.009	0.027			•		•			·			-	
	P	0.926	1.000	0.577	0.642	0.022	1.000	0.082	0.201	1.000	0.795	0.212	1.000	0.696	0.497	1.000	1.000	0.253	1.000	0.317	1.000	1.000	1.000
	S1	n/d	n/d	0.931	0.853	n/d	n/d	n/d	n/d	n/d	0.659	n/d	n/d	n/d	n/d	n/d	0.731	n/d	n/d	n/d	n/d	n/d	0.780
	R1	0.391	0.895	0.710	0.404	1.000	1.000	0.477	1.000	1.000	0.260	1.000	1.000	1.000	1.000	1.000	0.577	1.000	1.000	1.000	1.000	1.000	1.000
	S2	n/d	n/d	0.780	0.853	n/d	n/d	n/d	n/d	n/d	0.043	n/d	n/d	n/d	n/d	n/d	0.228	n/d	n/d	n/d	n/d	n/d	0.096
	R2	0.458	0.238	0.853	0.642	1.000	0.082	0.137	1.000	0.016	< 0.001	0.423	0.256	1.000	1.000	0.053	0.016	1.000	0.833	0.163	1.000	0.581	0.002
	S3	0.710	0.358	0.516	0.458	0.656	1.000	1.000	1.000	0.066	0.351	0.423	1.000	1.000	1.000	0.253	1.000	1.000	1.000	0.990	1.000	0.677	0.990
	R3	0.780	0.793	0.458	0.780	0.895	0.001	0.000	0.420	0.004	0.260	1.000	0.016	0.001	0.497	0.080	1.000	1.000	0.062	< 0.001	1.000	0.098	0.317

RWC leaf 8	all time	0.269	0.948	0.848	0.032	0.002	< 0.001	0.386	0.044	0.095	< 0.001												
	P	0.919	0.772	0.682	0.414	1.000	1.000	0.588	1.000	0.758	0.898	1.000	1.000	1.000	1.000	1.000	1.000	1.000	1.000	0.760	1.000	0.686	1.000
	S1	n/d	n/d	1.000	0.759	n/d	n/d	n/d	n/d	n/d	0.188	n/d	n/d	n/d	n/d	n/d	0.298	n/d	n/d	n/d	n/d	n/d	0.414
•	R1	0.479	0.470	0.838	0.262	1.000	0.005	1.000	0.117	1.000	0.005	1.000	0.026	1.000	1.000	1.000	0.016	1.000	0.313	1.000	0.280	1.000	0.503
	S2	n/d	n/d	1.000	1.000	n/d	n/d	n/d	n/d	n/d	0.010	n/d	n/d	n/d	n/d	n/d	0.067	n/d	n/d	n/d	n/d	n/d	0.067
	R2	0.474	0.772	0.540	0.609	0.073	< 0.001	1.000	0.086	0.027	1.000	0.339	< 0.001	1.000	0.580	0.231	1.000	0.580	< 0.001	1.000	0.408	0.280	< 0.001
	S3	0.838	0.664	0.682	0.682	0.045	0.007	1.000	1.000	0.002	< 0.001	0.231	0.255	1.000	1.000	0.019	0.011	0.488	0.052	1.000	1.000	0.189	0.011
	R3	0.262	0.312	0.084	0.012	0.053	< 0.001	< 0.001	< 0.001	0.027	0.371	0.488	< 0.001	< 0.001	< 0.001	0.686	0.004	0.280	< 0.001	< 0.001	0.408	0.080	1.000
RWC leaf 12	all time points	0.280	0.306	0.071	0.351	0.001	< 0.001	0.015	0.435	0.769	< 0.001	-		-	-	-	-	-		-	-	-	
	P	0.938	0.827	0.487	0.487	1.000	1.000	0.618	1.000	1.000	1.000	1.000	1.000	1.000	1.000	1.000	1.000	1.000	1.000	0.863	1.000	1.000	1.000
	S1	n/d	n/d	0.617	0.817	n/d	n/d	n/d	n/d	n/d	0.916	n/d	n/d	n/d	n/d	n/d	0.775	n/d	n/d	n/d	n/d	n/d	0.643
	R1	0.373	0.051	0.106	0.589	1.000	0.980	1.000	1.000	1.000	0.767	1.000	1.000	1.000	1.000	1.000	1.000	1.000	1.000	1.000	1.000	1.000	0.639
	S2	n/d	n/d	0.643	0.817	n/d	n/d	n/d	n/d	n/d	0.035	n/d	n/d	n/d	n/d	n/d	0.166	n/d	n/d	n/d	n/d	n/d	0.106
	R2	0.589	0.743	0.248	1.000	0.502	< 0.001	1.000	0.146	1.000	0.003	0.616	0.011	1.000	1.000	1.000	0.331	1.000	0.001	1.000	0.147	1.000	0.015
	S3	0.643	0.743	0.757	0.699	0.104	0.006	1.000	1.000	0.341	0.036	0.234	0.087	1.000	1.000	1.000	0.639	1.000	0.131	1.000	1.000	1.000	0.131
	R3	0.699	0.445	0.938	0.106	0.116	< 0.001	< 0.001	0.006	1.000	0.016	1.000	< 0.001	0.192	0.038	1.000	0.023	0.314	< 0.001	0.005	0.314	1.000	0.995
Relative leaf expansion rate (RLER)	S3	0.997	n/d	0.881	0.608	n/d	0.001	< 0.001	n/d	n/d	1.000	n/d	0.017	0.003	n/d	n/d	1.000	n/d	0.024	0.010	n/d	n/d	1.000
Area per leaf	S3	0.495	n/d	0.436	0.896	n/d	0.002	0.002	n/d	n/d	1.000	n/d	0.030	0.014	n/d	n/d	1.000	n/d	0.024	0.048	n/d	n/d	1.000
Cell number	S3	0.368	n/d	0.877	0.371	n/d	0.072	0.270	n/d	n/d	1.000	n/d	0.142	0.747	n/d	n/d	1.000	n/d	0.565	0.578	n/d	n/d	1.000
Cell size	S3	0.672	n/d	0.586	0.366	n/d	0.002	< 0.001	n/d	n/d	1.000	n/d	0.027	0.002	n/d	n/d	0.643	n/d	0.021	0.032	n/d	n/d	1.000
Carbon sum	all time points	0.579	0.634	0.391	0.344	0.790	1.000	0.021	0.086	0.002	0.268	0.664	1.000	0.675	0.499	0.041	0.941	1.000	0.819	0.044	0.369	0.024	0.804
Anthocyanin index (ANTH)	all time points	0.216	0.780	0.632	0.690	< 0.001	0.047	1.000	0.336	< 0.001	0.001				-	-						-	-
	P	0.676	0.426	0.516	0.552	1.000	0.775	1.000	1.000	0.837	0.035	1.000	1.000	1.000	1.000	1.000	1.000	1.000	1.000	1.000	1.000	1.000	1.000
	R1	0.419	0.308	0.565	0.357	0.621	1.000	1.000	1.000	0.050	0.265	0.102	1.000	1.000	0.703	0.016	0.657	1.000	1.000	1.000	1.000	1.000	1.000
	R2	0.693	0.283	0.867	0.850	0.001	0.287	1.000	0.227	< 0.001	0.056	0.008	0.774	1.000	0.263	0.005	0.560	0.244	1.000	1.000	1.000	0.040	0.257
	S3	0.675	0.920	0.685	0.804	0.192	1.000	1.000	0.354	0.157	1.000	0.470	1.000	1.000	1.000	0.775	1.000	1.000	1.000	1.000	0.754	0.602	1.000
	R3	0.491	0.339	0.894	0.889	1.000	0.840	1.000	1.000	1.000	0.345	1.000	1.000	1.000	1.000	1.000	1.000	1.000	1.000	1.000	1.000	0.735	0.820
Flavonol index (FLAV)	all time points	0.203	0.900	0.834	0.591	0.002	0.163	1.000	0.490	0.015	0.848					-							-
	P	0.538	0.668	0.393	0.752	1.000	1.000	1.000	1.000	1.000	1.000	1.000	1.000	1.000	1.000	1.000	1.000	1.000	1.000	1.000	1.000	1.000	1.000
	R1	0.049	0.902	0.933	0.295	0.354	1.000	1.000	1.000	0.722	1.000	0.133	0.652	1.000	1.000	0.504	1.000	1.000	1.000	1.000	1.000	1.000	1.000
	R2	0.839	0.807	0.792	0.955	0.156	0.347	1.000	1.000	0.739	1.000	0.886	1.000	1.000	1.000	1.000	1.000	0.489	1.000	1.000	1.000	1.000	1.000
	S3	0.731	0.483	0.471	0.981	0.071	1.000	1.000	0.554	0.286	1.000	0.080	1.000	1.000	1.000	0.326	1.000	1.000	1.000	1.000	1.000	1.000	1.000
	R3	0.549	0.543	0.825	0.860	1.000	1.000	1.000	1.000	1.000	1.000	1.000	1.000	1.000	1.000	1.000	1.000	1.000	1.000	1.000	1.000	1.000	1.000
Nitrogen balance index (NBI)	all time points	0.348	0.512	0.320	0.614	0.066	0.119	0.107	1.000	1.000	1.000												
	P	0.585	0.647	0.756	0.974	1.000	0.645	0.616	1.000	1.000	1.000	1.000	1.000	0.948	1.000	1.000	1.000	1.000	1.000	1.000	1.000	1.000	1.000
	R1	0.650	0.942	0.566	0.715	1.000	1.000	1.000	1.000	1.000	1.000	1.000	1.000	1.000	1.000	1.000	1.000	1.000	1.000	1.000	1.000	1.000	1.000
	R2	0.619	0.851	0.370	0.738	0.343	1.000	1.000	1.000	1.000	1.000	0.797	1.000	1.000	1.000	1.000	1.000	1.000	1.000	1.000	1.000	1.000	1.000
	S3	0.658	0.658	0.746	0.829	1.000	0.574	1.000	0.575	1.000	1.000	1.000	1.000	1.000	1.000	1.000	1.000	1.000	1.000	1.000	1.000	1.000	1.000
	R3	0.872	0.758	0.896	0.857	1.000	1.000	1.000	1.000	1.000	1.000	1.000	1.000	1.000	1.000	1.000	1.000	1.000	1.000	1.000	1.000	1.000	1.000
Chlorophyll index (SFR)	all time points	0.049	0.331	0.176	0.123	0.078	1.000	1.000	0.888	0.761	1.000					-							
	P	0.529	0.802	0.771	0.955	1.000	1.000	1.000	1.000	1.000	1.000	1.000	1.000	1.000	1.000	1.000	1.000	1.000	1.000	1.000	1.000	1.000	1.000
	R1	0.284	0.954	0.556	0.209	1.000	1.000	1.000	1.000	1.000	1.000	1.000	1.000	1.000	1.000	1.000	1.000	1.000	1.000	1.000	1.000	1.000	1.000

	R2	0.502	0.950	0.510	0.444	0.167	1.000	1.000	0.172	1.000	1.000	0.375	1.000	1.000	0.388	1.000	1.000	1.000	1.000	1.000	1.000	1.000	1.000
	S3	0.634	0.407	0.185	0.639	1.000	0.938	1.000	1.000	1.000	1.000	1.000	1.000	1.000	1.000	1.000	1.000	1.000	0.770	1.000	1.000	1.000	1.000
	R3	0.203	0.276	0.908	0.308	1.000	1.000	1.000	1.000	1.000	1.000	1.000	1.000	1.000	1.000	1.000	1.000	1.000	1.000	1.000	1.000	1.000	1.000
Γemperature (leaf)	all time points	0.659	0.864	0.553	0.559	1.000	0.830	< 0.001	1.000	< 0.001	< 0.001						. !						-
	P	0.710	0.713	0.933	0.888	1.000	1.000	1.000	1.000	1.000	1.000	1.000	1.000	1.000	1.000	1.000	1.000	1.000	1.000	1.000	1.000	1.000	1.000
	R1	0.531	0.926	0.615	0.638	1.000	1.000	< 0.001	1.000	< 0.001	< 0.001	1.000	1.000	< 0.001	1.000	< 0.001	< 0.001	1.000	1.000	< 0.001	1.000	< 0.001	< 0.00
	S2	n/d	n/d	0.931	0.955	1.			4 1		0.615	l .			4		0.669	1.					0.776
	R2	0.592	0.731	0.680	0.572	1.000	0.657	< 0.001	0.051	< 0.001	< 0.001	1.000	1.000	< 0.001	0.332	0.003	< 0.001	1.000	1.000	0.006	0.385	0.044	< 0.00
	S3	0.548	0.793	n/d.	n/d.	0.022	4.		4			0.072			4			0.141					
	R3	0.929	0.662	0.724	0.918	1.000	0.805	0.396	1.000	1.000	1.000	1.000	1.000	1.000	1.000	1.000	1.000	1.000	1.000	1.000	1.000	1.000	1.000
tem water potential (mid-day)	all time	0.240	0.384	0.656	0.447	0.329	0.011	< 0.001	1.000	< 0.001	0.002						. !					•	
	S3	0.250	0.844	0.650	0.473	1.000	< 0.001	< 0.001	0.006	< 0.001	0.002	1.000	0.002	< 0.001	0.044	< 0.001	0.034	0.808	< 0.001	< 0.001	0.194	< 0.001	0.068
	R3	0.230	0.844	0.860	0.473	0.839	1.000	1.000	0.000	1.000	0.002	1.000	1.000	1.000	1.000	1.000	1.000	0.808	1.000	1.000	0.194	0.651	1.000
	N.J	0.000	U.441	0.000	0.720	0.657	1.000					1.000	1.000	1.000	1.000	1.000	1.000	0.550	1.000	1.000	0.005	0.051	1.00.
									Leaf-	<u>-leve</u>	<u>l</u>												
ranspiration (E)	all time	0.002	0.971	< 0.001	< 0.001	0.855	0.001	0.011	0.058	0.450	1.000												
	S3	0.055	0.804	0.975	0.695	0.049	< 0.001	< 0.001	0.001	< 0.001	1.000	0.043	< 0.001	< 0.001	0.023	0.019	1.000	1.000	0.002	< 0.001	0.041	0.012	1.000
	R3	0.263	0.184	0.390	0.079	1.000	1.000	0.077	1.000	0.352	0.699	1.000	1.000	0.216	1.000	0.708	0.706	1.000	1.000	0.845	1.000	1.000	1.000
	all time											*	****	V	•		,		****	0.0	****	*****	
Net assimilation (A)	points	0.027	0.016	0.186	0.028	0.649	1.000	1.000	0.219	0.098	1.000			÷	-		. '		÷		•		•
	S3	0.050	0.099	0.531	0.418	1.000	< 0.001	< 0.001	< 0.001	< 0.001	1.000	1.000	0.001	< 0.001	0.002	0.001	1.000	1.000	0.047	0.008	0.046	0.008	1.000
	R3	0.225	0.071	0.212	0.021	0.089	0.001	< 0.001	0.657	0.373	1.000	0.248	0.029	0.003	1.000	0.674	1.000	0.872	0.032	0.081	0.932	1.000	1.00
Water-use efficiency (WUE)	all time	0.784	0.710	0.123	0.220	0.033	< 0.001	< 0.001	< 0.001	0.001	1.000				1.						•	•	
	S3	0.749	0.532	0.063	0.241	0.074	< 0.001	< 0.001	< 0.001	< 0.001	1.000	0.150	< 0.001	< 0.001	0.002	0.001	1.000	1.000	0.001	< 0.001	0.071	0.005	1.00
	R3	0.749	0.921	0.755	0.571	0.827	0.001	0.290	0.634	1.000	1.000	1.000	0.115	0.517	1.000	1.000	1.000	1.000	0.001	1.000	1.000	1.000	1.00
~	all time											1.000	0.112	0.51.	1.00.	1.000	1.000	1.000	0.200	1.000	1.000	1.00.	***
Stomatal conductance (g _s)	points	0.033	0.270	0.773	0.116	0.812	0.002	0.023	0.164	0.804	1.000	0.025	. 0.001	. 2.001	0.045	. 0.020			. 0.004	2.001		2.020	
	S3	0.048	0.815	0.981	0.734	0.042	< 0.001	< 0.001	0.002	0.001	1.000	0.035	< 0.001	< 0.001	0.045	0.038	1.000	1.000	0.004	0.001	0.077	0.028	1.00
	R3	0.291	0.186	0.701	0.061	1.000	1.000	0.068	1.000	0.333	1.000	1.000	1.000	0.160	1.000	0.600	0.529	1.000	1.000	0.948	1.000	1.000	1.00
Intracellular [CO ₂] (c _i)	all time	0.847	0.905	0.346	0.985	< 0.001	1.000	1.000	< 0.001	0.002	1.000											-	
	points S3	0.875	0.726	0.299	0.576	0.099	0.341	0.119	< 0.001	< 0.001	1.000	0.837	0.318	0.840	0.006	0.025	1.000	0.299	1.000	0.376	0.045	0.002	1.00
	R3	0.875	0.726	0.299	0.576	< 0.001	0.341	0.119	0.410	1.000	1.000	0.837	0.318	0.840	0.006	1.000	1.000	0.299	0.343	0.376	1.000	1.000	1.00
	all time	0.909	0.830	0.709	0.556	< 0.001	0.104	0.002	0.410	1.000	1.000	0.020	0.783	0.136	0.730	1.000	1.000	0.024	0.343	0.022	1.000	1.000	1.00
c_i/c_a		0.495	0.171	< 0.001	< 0.001	1.000	0.002	0.011	< 0.001	< 0.001	1.000												
	points S3	0.979	0.735	0.253	0.757	1.000	< 0.001	< 0.001	< 0.001	< 0.001	1.000	1.000	< 0.001	0.001	0.001	0.002	1.000	1.000	0.015	< 0.001	0.013	< 0.001	1.00
	R3	0.715	0.733	0.233	0.737	0.395	1.000	0.987	0.331	1.000	0.851	0.956	1.000	1.000	0.001	1.000	1.000	1.000	1.000	1.000	1.000	1.000	1.00
	all time					0.373	1.000	0.507	0.551	1.000	0.651	0.750	1.000	1.000	0.554	1.000	1.000	1.000	1.000	1.000	1.000	1.000	1.0.
Γranspiration dark (E _d)	points	0.593	0.798	0.429	0.221	-					. I	-					. !	-	-		-		-
	S3	0.378	0.606	0.769	0.938	0.865	< 0.001	< 0.001	0.023	0.031	1.000	0.515	0.002	0.004	0.280	0.424	1.000	1.000	0.072	0.068	0.168	0.159	1.00
	R3	0.898	0.876	0.409	0.073	0.536	0.001	< 0.001	0.181	< 0.001	0.022	1.000	0.107	< 0.001	< 0.001	< 0.001	0.006	1.000	0.016	0.001	0.261	0.033	1.00
Respiration dark (R _d)	all time points	0.509	0.309	0.456	0.830	0.843	0.361	0.001	1.000	0.061	0.175				-		. !						-
	S3	0.060	0.987	0.352	0.920	1.000	1.000	1.000	1.000	1.000	0.607	1.000	1.000	1.000	1.000	1.000	1.000	1.000	0.185	1.000	1.000	1.000	0.69
											_	1					0.210	0.876	0.001		_		

Isoprene emission, leaf-level	all time points	< 0.001	0.000	< 0.001	< 0.001	0.039	1.000	1.000	0.064	0.855	1.000		-		-	-		-	-		-		
	S3	< 0.001	0.001	< 0.001	< 0.001	0.466	1.000	1.000	0.155	1.000	1.000	0.114	1.000	1.000	0.018	0.950	0.581	1.000	1.000	1.000	1.000	1.000	1.000
	R3	< 0.001	0.002	< 0.001	< 0.001	0.199	1.000	1.000	0.906	1.000	1.000	0.476	1.000	1.000	0.316	0.772	1.000	1.000	1.000	1.000	1.000	1.000	1.000
Photosynthetic carbon lost as isoprene (C%)	all time points	< 0.001	0.044	< 0.001	< 0.001	1.000	0.418	0.318	0.013	0.009	1.000	-	-		-	-		-	-	-	-	-	
	S3	0.020	0.124	< 0.001	< 0.001	1.000	0.010	0.002	0.001	< 0.001	1.000	1.000	< 0.001	< 0.001	< 0.001	< 0.001	1.000	1.000	1.000	1.000	1.000	1.000	1.000
	R3	0.004	0.180	0.042	0.091	1.000	1.000	1.000	1.000	1.000	1.000	0.560	1.000	1.000	1.000	1.000	1.000	1.000	1.000	1.000	1.000	1.000	1.000
Net ecosystem productivity	all time points	0.191	0.630	0.687	0.056	0.126	1.000	0.062	1.000	0.010	0.002					-		-					
	P	0.137	0.840	0.030	0.569	1.000	0.141	1.000	1.000	0.644	0.006	1.000	1.000	1.000	1.000	1.000	1.000	1.000	0.299	0.414	0.637	0.823	0.002
	S3	0.482	0.740	0.711	0.518	1.000	0.002	< 0.001	< 0.001	< 0.001	0.103	1.000	0.216	0.002	0.019	< 0.001	0.696	1.000	0.012	< 0.001	0.023	< 0.001	0.395
	R3	0.943	0.482	0.013	0.035	0.188	< 0.001	< 0.001	0.049	0.183	1.000	0.302	< 0.001	< 0.001	0.076	0.276	1.000	1.000	0.026	0.052	1.000	1.000	1.000
Net isoprene loss	all time points	0.000	0.059	< 0.001	0.000	1.000	0.153	0.003	0.022	0.001	0.930						-					-	
	P	0.042	0.559	0.030	0.026	1.000	1.000	1.000	1.000	1.000	1.000	1.000	1.000	1.000	1.000	1.000	1.000	1.000	1.000	1.000	1.000	1.000	1.000
	S3	0.022	0.381	0.000	< 0.001	1.000	0.002	< 0.001	0.002	< 0.001	0.964	1.000	< 0.001	< 0.001	< 0.001	< 0.001	0.215	1.000	1.000	1.000	1.000	1.000	1.000
	R3	0.002	0.068	0.003	< 0.001	1.000	1.000	1.000	1.000	1.000	1.000	1.000	1.000	0.460	1.000	0.314	0.295	1.000	1.000	1.000	1.000	1.000	1.000

5

8

10 11

Table S2. Calculated angles of different stress phases of cumulative net C gain. Phases are: P = pre-stress, S1 = stress cycle 1, R1 = recovery phase

7 1, S2 = stress cycle 2, R2 = recovery phase 2, S3 = stress cycle 3, R3 = recovery phase 3. In CS scenario, the phases are named as follows: P = pre-

stress, S_{IN} = stress initial, S_{SEV} = stress severe, R = recovery. The scenarios are: AC = control with ambient $[CO_2]$, EC = control with elevated

9 [CO₂], PS = periodic stress, CS =

chronic stress. IE = isoprene-

emitting, NE = non-emitting.

AC			EC			PS			CS		
	IE	NE		IE	NE		IE	NE		IE	NE
P	27.5°	30.0°	P	29.0°	29.0°	P	38.0°	38.0°	P	38.0°	37.5°
						S1	20.0°	21.0°	$S_{\rm IN}$	25.0°	22.0°
						R1	39.0°	39.0°	S_{SEV}	15.5°	12.0°
						S2	9.0°	10.0°	R	43.5°	42.0°
						R2	39.5°	37.0°			
						R3	16.0°	14.0°			
						R3	42.5°	36.0°			